Supporting Information

Topology Exploration in Highly Connected Rare-Earth Metal–Organic Frameworks via Continuous Hindrance Control

Yutong Wang[†,‡], Liang Feng[§,‡], Weidong Fan[†], Kun-Yu Wang[§], Xia Wang[†], Xiaokang Wang[†], Kai Zhang[†], Xiurong Zhang[†], Fangna Dai[†], Daofeng Sun[*†], and Hong-Cai Zhou[*§#]

[†] School of Materials Science and Engineering, College of Science, China University of Petroleum (East China), Qingdao, Shandong 266580, China

[§] Department of Chemistry, Texas A&M University, College Station, Texas 77843-3255, United States

[#] Department of Materials Science and Engineering, Texas A&M University, College Station, Texas 77843-3003, United States

[‡] These authors contributed equally to this work.

Corresponding Authors:

*dfsun@upc.edu.cn

*zhou@chem.tamu.edu

Contents

S1.Ligand Synthesis

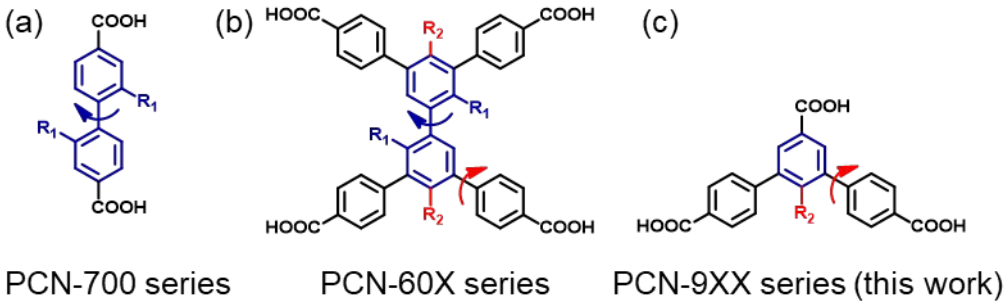

Figure S1. Tuning linker configuration through the introduction of steric hindrance in PCN-700 series (a), PCN-60X series (b) and PCN-9XX series (c, this work).

Synthesis of H_3L-R (R = -H, -F, -OCH_3, -NH_2, -CH_3, -Cl)

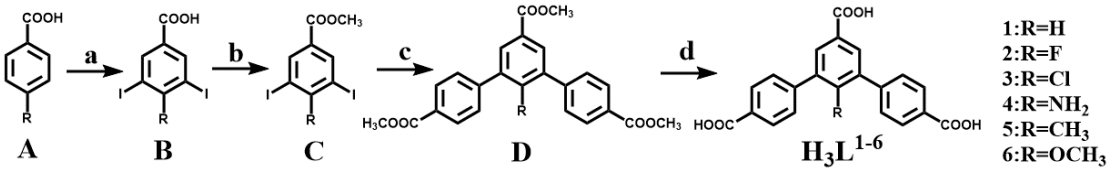

Synthesis of H_3L-H and H_3L-NH_2

H_3L-H and H_3L-NH_2 were prepared according to the reported procedures.[1]

Synthesis of H_3L-F

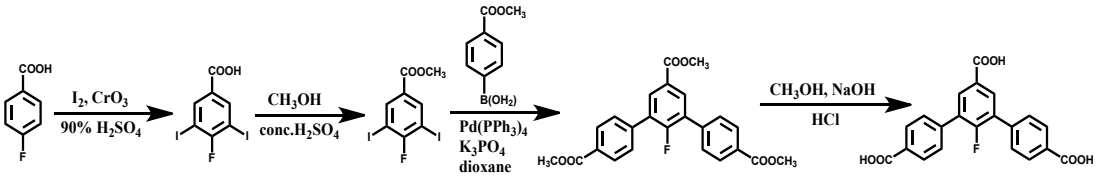

Scheme S1. Synthetic procedure for **H_3L-F**.

(1) 4-fluoro-3,5-diiodobenzoic acid

CrO_3 (2.0g, 20.0 mmol) and finely powdered iodine (5.08 g, 20.0mmol) were added into H_2SO_4 (90%, 100ml, V/V) solution. The mixture was stirred at 30 °C for 30 min, following by the addition of 4-fluorobenzoic acid (2.10 g, 15.0 mmol). The mixture was stirred at 25-30 °C for 24 h and then poured into ice/water and collected via vacuum filtration. The solid was washed with cool water and then dried *in vacuo* at 50 °C. The crude (3.41 g, 58%) material was collected as a white solid, which was used without further purification. ^{1}H NMR (400 MHz, $CDCl_3$) δ 8.42 (s, 2 H), 12.74(s, H) ppm.

(2) Methyl 4-amino-3,5-diiodobenzoate

4-fluoro-3,5-diiodobenzoic acid (19.6 g, 50.0 mmol) was suspended in 200 ml methanol at room temperature. Concentrated H_2SO_4 (9.5ml) was added slowly with rapid stirring and then the reaction mixture was heated under reflux for 48 h. TLC (silica, CH_2Cl_2) was utilized to indicate the complete consumption of the starting materials. The solution was cooled down to room temperature, and then product [18.87 g (93%)] was precipitated in an ice bath. ^{1}H NMR (400 MHz, $CDCl_3$) δ 3.88 (s, 3 H), 8.32 (s, 2 H) ppm. Anal. Calc. for $C_8H_5I_2FO_2$ (mw 406): C, 23.65; H 1.23. Found: C, 23.63; H, 1.21.

(3) Trimethyl 2'-fluoro-[1,1':3',1''-terphenyl]-4,4'',5'-tricarboxylate

Methyl 4-amino-3,5-diiodobenzoate (1.62 g, 4 mmol), methyl 4-boronobenzoate (1.57 g, 9.6 mmol), $Pd(PPh_3)_4$ (0.15 g, 0.13 mmol) and K_3PO_4 (3.82 g, 18.0 mmol) were placed in a 500 ml two-necked round bottom flask under N_2 atmosphere. The flask was further charged with 200 mL of dry 1,4-dioxane, and heated for 48 h. After the mixture was cooled down to room temperature, the solvent was removed and water was added. The water phase was washed with CH_2Cl_2 while the mixed organic phase was further dried by $MgSO_4$. After the solvent was removed, the crude product was purified by column chromatography with CH_2Cl_2 as the eluent. ^{1}H NMR (400 MHz, $CDCl_3$) δ 3.87(s, 3H), 3.96(s, 6H), 7.81(d, 4H), 8.16(s, 2H), 8.29(d, 4H) ppm. Anal. Calc. for $C_{24}H_{19}FO_6$ (mw 422): C, 68.25; H, 4.50. Found: C, 68.27; H, 4.55.

(4) 2'-fluoro-[1,1':3',1''-terphenyl]-4,4'',5'-tricarboxylic acid

Trimethyl 2'-fluoro-[1,1':3',1''-terphenyl]-4,4'',5'-tricarboxylate (2.0 g, 4.7 mmol) was dissolved in 50 mL MeOH, following by the addition of 50 mL 2 M NaOH aqueous solution. The mixture was stirred at 50 °C overnight. The organic phase was removed, and the aqueous phase was acidified with dilute hydrochloric acid. The yellow precipitate was filtered and washed with water for several times. ^{1}H NMR (400 MHz, DMSO-d6) δ 7.66(d, 4H), 7.94(s, 2H), 8.06(d, 4H), 12.78(s, 3H) ppm. Anal. Calc. for $C_{21}H_{15}NO_6$ (mw 377): C, 66.84; N, 3.71; H, 4.01. Found: C, 66.78; N, 3.73; H, 4.00.

Synthesis of H_3L-Cl

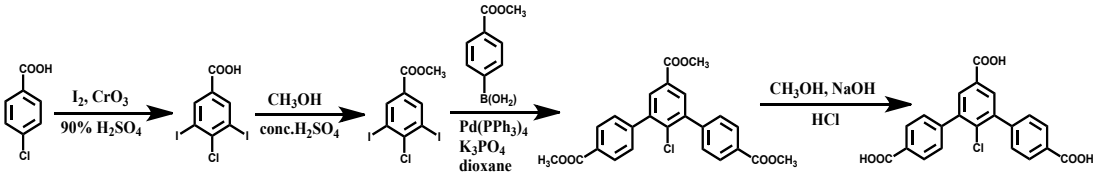

Scheme S2. Synthetic procedures of the **H_3L-Cl**.

(1) 4-chloro-3,5-diiodobenzoic acid

CrO_3 (2.0g, 20.0 mmol) and finely powdered iodine (5.08 g, 20.0mmol) were added into H_2SO_4 (90%, 100ml, V/V) solution. The mixture was stirred at 30 °C for 30 min, following by the addition of 4-chlorobenzoic acid (2.34 g, 15.0 mmol). The mixture was stirred at 25-30 °C for 24 h and then poured into ice/water and collected via vacuum filtration. The solid was washed with cool water and then dried *in vacuo* at 50 °C. The crude (4.28 g, 70%) material was collected as a white solid which was used without further purification. ^{1}H NMR (400 MHz, $CDCl_3$) δ 8.44 (s, 2 H), 12.74(s, H) ppm.

(2) Methyl 4-chloro-3,5-diiodobenzoate

4-chloro-3,5-diiodobenzoic acid (20.4 g, 50.0 mmol) was suspended in 200 mL methanol at room temperature. Concentrated H_2SO_4 (9.5 mL) was added slowly with rapid stirring, followed by heating under reflux for 48 h. TLC (silica, CH_2Cl_2) was utilized to indicate the complete consumption of the starting materials. The solution was initially cooled down to room temperature, and the white product [20.7 g (98%)] was precipitated in an ice bath. ^{1}H NMR (400 MHz, $CDCl_3$) δ 3.88 (s, 3 H), 8.28 (s, 2 H) ppm. Anal. Calc. for $C_8H_5I_2ClO_2$ (mw 422): C, 22.75; H, 1.18. Found: C, 22.76; H, 1.11.

(3) Trimethyl 2'-chloro-[1,1':3',1''-terphenyl]-4,4'',5'-tricarboxylate

Methyl 4-chloro-3,5-diiodobenzoate (1.69 g, 4 mmol), methyl 4-boronobenzoate (1.57 g, 9.6 mmol), $Pd(PPh_3)_4$ (0.15 g, 0.13 mmol) and K_3PO_4 (3.82 g, 18.0 mmol) were placed in a 500 ml two-necked round bottom flask under N_2 gas atmosphere. The flask was further charged with 200 mL dry 1,4-dioxane, and heated for 48 h. After the mixture was cooled down to room temperature, the solvent was removed and water was added. The water phase was washed with CH_2Cl_2. The mixed organic phase was dried by $MgSO_4$. After the solvent was removed, the crude product was purified by column chromatography with CH_2Cl_2 as the eluent. ^{1}H NMR (400 MHz, $CDCl_3$) δ 3.87(s, 3H), 3.96(s, 6H), 7.80(d, 4H), 8.12(s, 2H), 8.21(d, 4H) ppm. Anal. Calc. for $C_{24}H_{19}ClO_6$ (mw

438): C, 65.75; H, 4.34. Found: C, 65.80; H, 4.30.

(4) 2'-chloro-[1,1':3',1''-terphenyl]-4,4'',5'-tricarboxylic acid

Trimethyl 2'-chloro-[1,1':3',1''-terphenyl]-4,4'',5'-tricarboxylate (2.0 g, 4.6 mmol) was dissolved in 50 mL MeOH, followed by the addition of 50 mL 2 M NaOH aqueous solution. The mixture was stirred at 50 °C overnight. The organic phase was removed, and the aqueous phase was acidified with dilute hydrochloric acid. The yellow precipitate was filtered and washed with water several times. ^{1}H NMR (400 MHz, DMSO-d6) δ 7.64(d, 4H), 7.93(s, 2H), 8.05(d, 4H), 13.21(s, 3H) ppm. Anal. Calc. for $C_{21}H_{13}ClO_6$ (mw 396): C, 63.64; H, 3.28. Found: C, 63.68; H, 3.23.

Synthesis of H_3L-CH_3

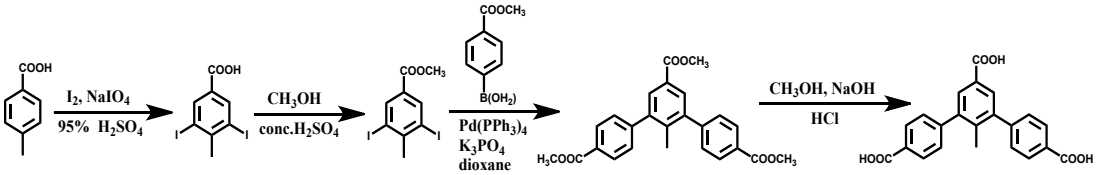

Scheme S3. Synthetic procedures of the **H_3L-CH_3**.

(1) 3,5-diiodo-4-methylbenzoic acid

$NaIO_4$ (0.34 g, 1.59mmol) and finely powdered iodine (1.20 g, 4.73 mmol) were added in H_2SO_4 (95%, 30 mL, V/V) solution. The mixture was stirred at 30 °C for 30 min, followed by the addition of 4-methylbenzoic acid (2.04 g, 15.0 mmol). The mixture was stirred at 30 °C for 2 h and then poured into ice/water and filtered by a vacuum. The solid was washed with cool water and then dried by vacuum at 50 °C. The material was further recrystallized with ethanol, affording a white solid (3.43 g, 59%). ^{1}H NMR (400 MHz, $CDCl_3$) δ 3.36 (s, 3 H),8.44 (s, 2 H), 12.74 (s, H) ppm.

(2) Methyl 3,5-diiodo-4-methylbenzoate

3,5-diiodo-4-methylbenzoic acid (19.39 g, 50.0 mmol) was suspended in 200 mL methanol at room temperature. Concentrated H_2SO_4 (9.5ml) was added slowly with rapid stirring followed by heating under reflux for 48 h. TLC (silica, CH_2Cl_2) was utilized to indicate the complete consumption of the starting materials. The solution was cooled down to room temperature and then the product [19.08 g (95%)] was precipitated in an ice bath. ^{1}H NMR (400 MHz, $CDCl_3$) δ 3.36 (s, 3 H), 3.88 (s, 3 H), 8.22 (s, 2 H) ppm. Anal. Calc. for $C_9H_8I_2O_2$ (mw 402): C, 26.86; H, 1.99. Found: C,

26.79; H, 1.98.

(3) Trimethyl 2'-methyl-[1,1':3',1''-terphenyl]-4,4'',5'-tricarboxylate

Methyl 4-chloro-3,5-diiodobenzoate (1.61 g, 4 mmol), methyl 4-boronobenzoate (1.57 g, 9.6 mmol), $Pd(PPh_3)_4$ (0.15 g, 0.13 mmol) and K_3PO_4 (3.82 g, 18.0 mmol) were placed in a 500 mL two-necked round bottom flask under N_2 gas atmosphere. The flask was further charged with 200 mL dry 1,4-dioxane, and heated for 48 h. After the mixture was cooled down to room temperature, the solvent was removed and water was added. The water phase was washed with CH_2Cl_2. The mixed organic phase was further dried by $MgSO_4$. After the solvent was removed, the crude product was purified by column chromatography with CH_2Cl_2 as the eluent. ^{1}H NMR (400 MHz, $CDCl_3$) δ 3.87(s, 3H), 3.96(s, 6H), 7.75(d, 4H), 7.94(s, 2H), 8.46(d, 4H) ppm. Anal. Calc. for $C_{25}H_{22}O_6$ (mw 418): C, 71.76; H, 5.30. Found: C, 71.78; H, 5.25.

(4) 2'-methyl-[1,1':3',1''-terphenyl]-4,4'',5'-tricarboxylic acid

Trimethyl 2'-methyl-[1,1':3',1''-terphenyl]-4,4'',5'-tricarboxylate (2.0 g, 4.8 mmol) was dissolved in 50 mL of MeOH, followed by the addition of 50 mL 2 M NaOH aqueous solution. The mixture was stirred at 50 °C overnight. The organic phase was removed, while the aqueous phase was acidified with diluted hydrochloric acid. The yellow precipitate was filtered and washed with water for several times. ^{1}H NMR (400 MHz, DMSO-d6) δ 3.36 (s, 3H), 7.57(d, 4H), 7.80 (s, 2H), 8.04(d, 4H), 13.08(s, 3H) ppm. Anal. Calc. for $C_{22}H_{16}O_6$ (mw 376): C, 70.21; H, 4.29. Found: C, 70.18; H, 4.30.

Synthesis of H_3L-OCH_3

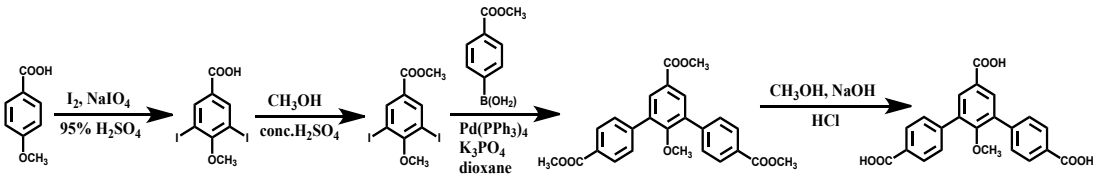

Scheme S4. Synthetic procedure for **H_3L-OCH_3**.

(1) 3,5-diiodo-4-methoxybenzoic acid

$NaIO_4$ (0.34 g, 1.59mmol) and finely powdered iodine (1.20 g, 4.73 mmol) were added in H_2SO_4 (95%, 30mL, V/V) solution. The mixture was stirred at 30 °C for 30 min followed by the addition of 4-methoxybenzoic acid (2.28 g, 15.0 mmol). The mixture was stirred at 30 °C for 2 h and then poured into ice/water and filtered by a vacuum.

The solid was washed with cool water and then dried by vacuum at 50 °C. Upon recrystallization with ethanol, a white solid was collected (3.82 g, 63%) and used without further purification. ^{1}H NMR (400 MHz, $CDCl_3$) δ 3.83(s, 3 H) 8.50 (s, 2 H), 12.74(s, H) ppm.

(2) Methyl 3,5-diiodo-4-methoxybenzoate

3,5-diiodo-4-methoxybenzoic acid (20.19 g, 50.0 mmol) was suspended in 200 mL methanol at room temperature. Concentrated H_2SO_4 (9.5ml) was added slowly with rapid stirring, followed by heating under reflux for 48 h. TLC (silica, CH_2Cl_2) was utilized to indicate the complete consumption of the starting materials. The solution was cooled down to room temperature, and then the white product [20.0 g (96%)] was precipitated in an ice bath. ^{1}H NMR (400 MHz, $CDCl_3$) δ 3.83 (s, 3 H), 3.89 (s, 3 H), 8.23 (s, 2 H) ppm. Anal. Calc. for $C_9H_8I_2O_3$ (mw 418): C, 25.86; H, 1.93. Found: C, 25.80; H, 1.91.

(3) Trimethyl 2'-methoxy-[1,1':3',1''-terphenyl]-4,4'',5'-tricarboxylate

Methyl 3,5-diiodo-4-methoxybenzoate (1.67 g, 4 mmol), methyl 4-boronobenzoate (1.57 g, 9.6 mmol), $Pd(PPh_3)_4$ (0.15 g, 0.13 mmol) and K_3PO_4 (3.82 g, 18.0 mmol) were placed in a 500 mL two-necked round bottom flask under N_2 gas atmosphere. The flask was further charged with 200 mL dry 1,4-dioxane, and heated for 48 h. After the mixture was cooled down to room temperature, the solvent was removed and water was added. The water phase was washed with CH_2Cl_2. The mixed organic phase was dried with $MgSO_4$. After the solvent was removed, the crude product was purified by column chromatography with CH_2Cl_2 as the eluent. ^{1}H NMR (400 MHz, $CDCl_3$) δ 3.83(s, 3H), 3.87(s, 3H), 3.96(s, 6H), 7.59(d, 4H), 7.84(s, 2H), 8.16(d, 4H) ppm. Anal. Calc. for $C_{23}H_{22}O_7$ (mw 434): C, 69.12; H, 5.10. Found: C, 69.20; H, 5.0.

(4) 2'-methoxy-[1,1':3',1''-terphenyl]-4,4'',5'-tricarboxylic acid

Trimethyl 2'-methoxy-[1,1':3',1"-terphenyl]-4,4",5'-tricarboxylate (2.0 g, 4.6 mmol) was dissolved in 50 mL MeOH followed by the addition of 50 mL of 2 M NaOH aqueous solution. The mixture was stirred at 50 °C overnight. The organic phase was removed, while the aqueous phase was acidified with dilute hydrochloric acid. The yellow precipitate was filtered and washed with water for several times. ^{1}H NMR (400 MHz, DMSO-d6) δ 2.50(s, 3H), 7.73(d, 4H), 7.96 (s, 2H), 8.05(d, 4H), 13.08(s, 3H) ppm. Anal. Calc. for $C_{22}H_{16}O_7$ (mw 392): C, 67.35; H, 4.11. Found: C, 67.28; H, 4.03.

S2.Optical and SEM Images

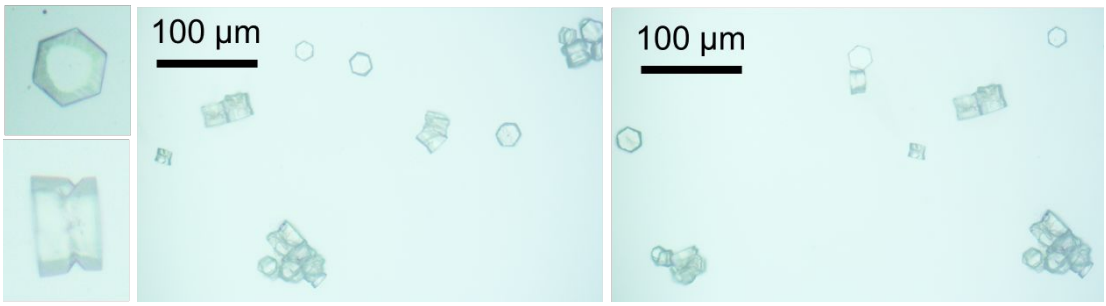

Figure S2. Optical images of PCN-909(Eu)-CH_3 with a hexagonal prism morphology.

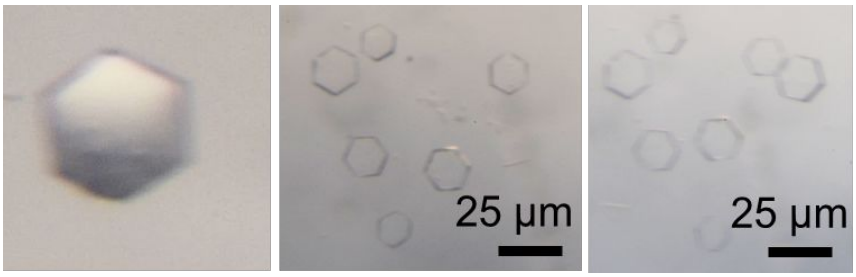

Figure S3. Optical images of PCN-909(Eu)-Cl with a hexagonal prism morphology.

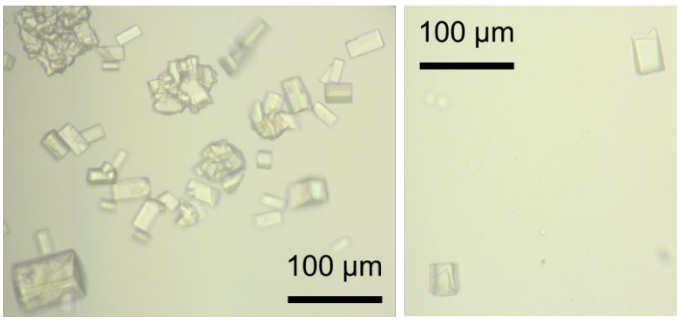

Figure S4. Optical images of PCN-912(Eu)-50%CH_3 with a cuboid morphology.

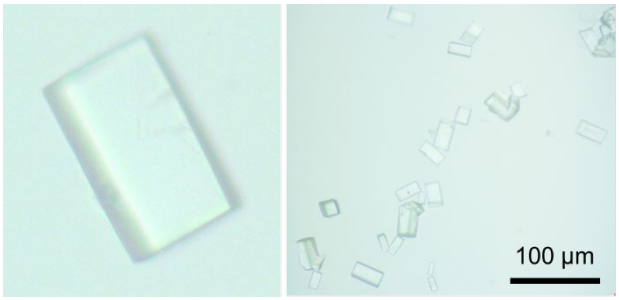

Figure S5. Optical images of PCN-918(Eu)-H with a cuboid morphology.

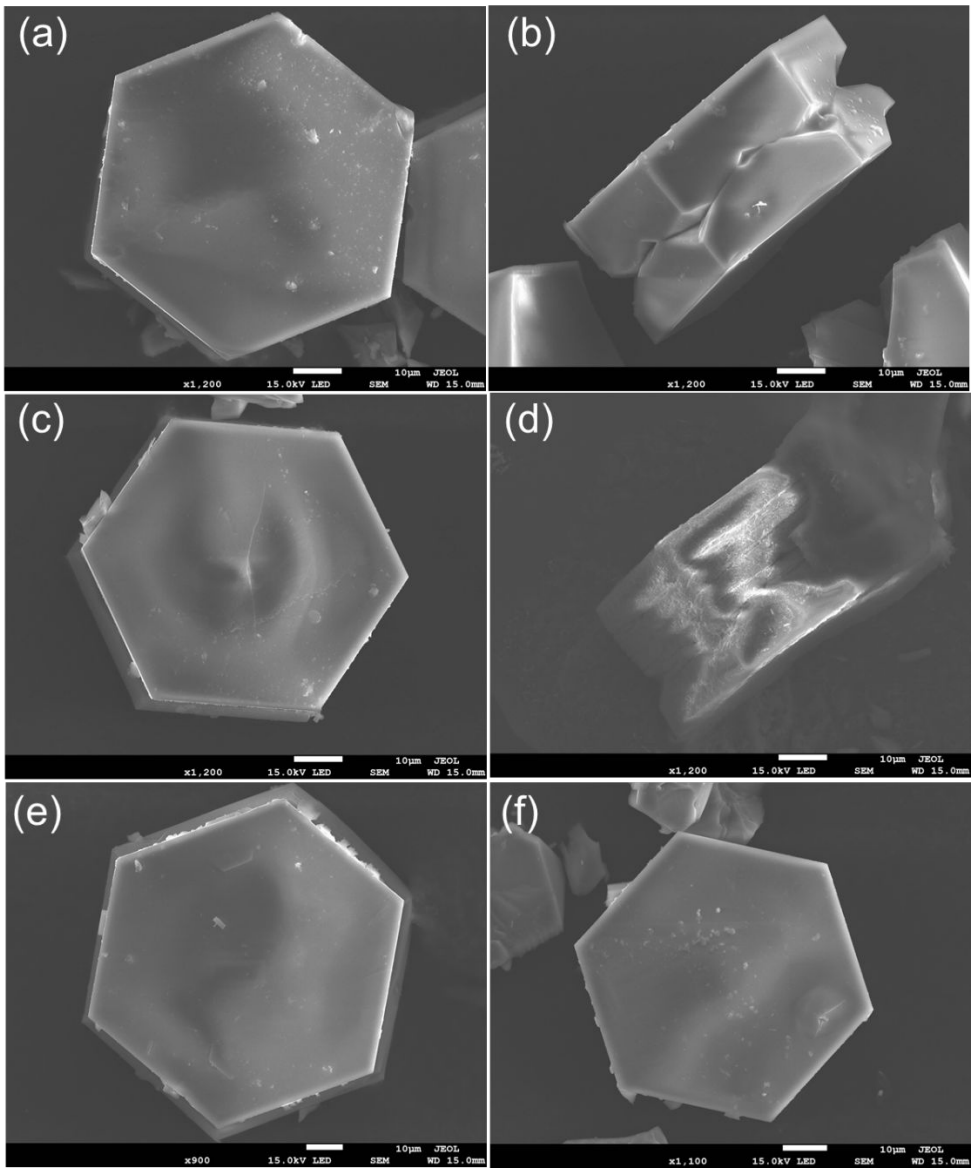

Figure S6. SEM images of PCN-909(Eu)-Cl before (a-b) and after solvent treatment: (c-d) water; (e) acetone; and (f) methanol.

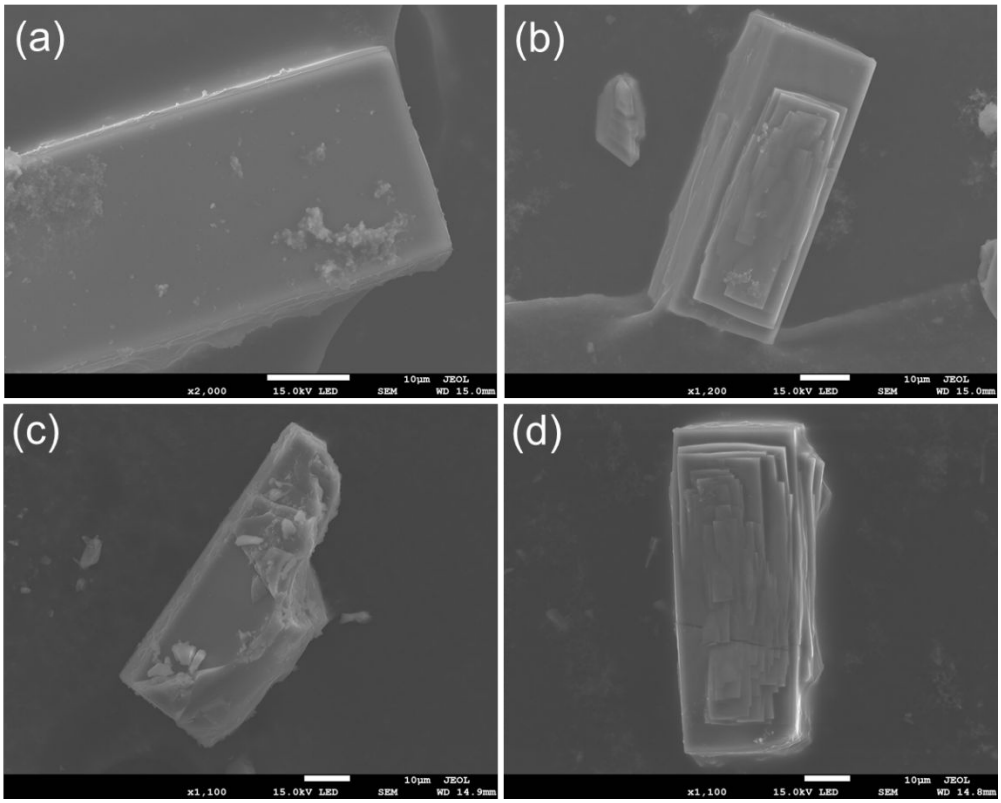

Figure S7. SEM images of PCN-912(Eu)-50%CH_3 before (a) and after solvent treatment: (b) water; (c) acetone; and (d) methanol.

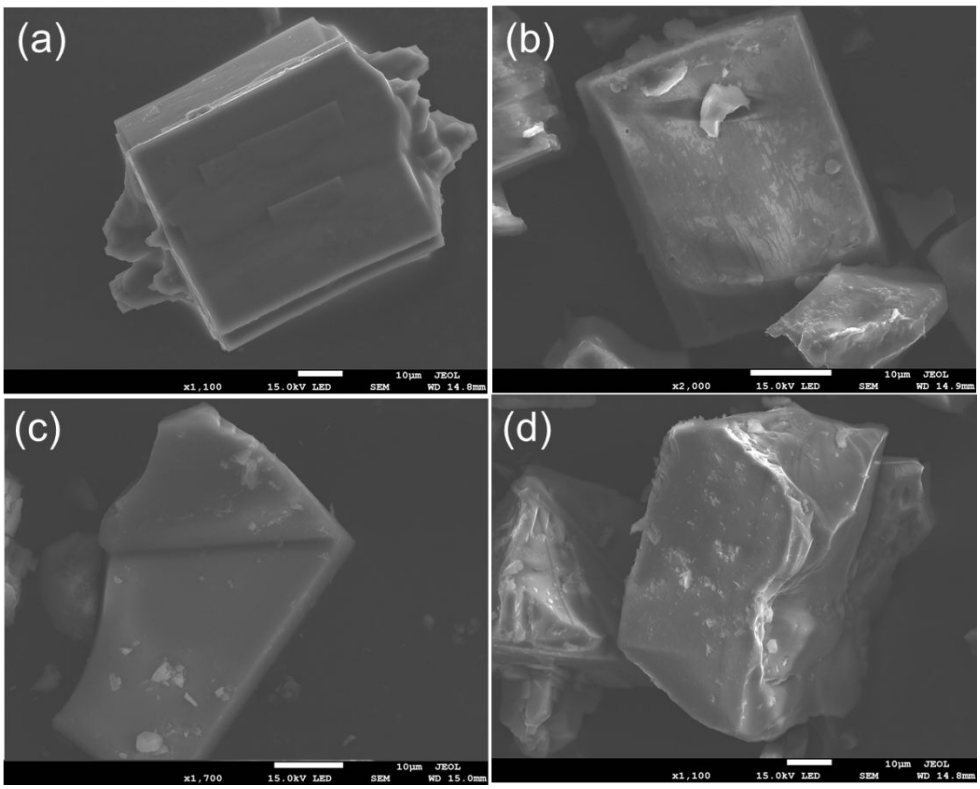

Figure S8. SEM images of PCN-918(Eu)-H before (a) and after solvent treatment: (b) water; (c) acetone; and (d) methanol.

S3. Single Crystal X-ray Crystallography

All as-synthesized crystals were taken from the mother liquid without further treatment. They were transferred to an oil environment and mounted onto a loop for single crystal X-ray data collection. All crystals data were collected with a SuperNova diffractometer equipped with mirror Cu-Kα radiation (λ = 1.54184 Å) and an Eos CCD detector at 150 K. The data was collected with a ω-scan technique and an arbitrary φ-angle. Data reductions were performed with the CrysAlisPro package, and an analytical absorption correction was performed. All the structures were solved by the direct method using the *SHELXS* program of the *SHELXTL* package and refined by the full-matrix least-squares method with *SHELXL*.[2] The structures were treated anisotropically, whereas the aromatic and hydroxyl hydrogen atoms were placed in calculated ideal positions and refined as riding on their respective carbon or oxygen atoms. Structure was examined using the Addsym subroutine of PLATON to assure that no additional symmetry could be applied to the models. Crystal data collection are summarized in Table S1, Supporting Information and crystal structures can be accessed in CCDC 1872204-1872208.

Table S1. Crystal data and structure refinements.

Name	PCN-909-Cl	PCN-909-NH_2	PCN-909-CH_3	PCN-912-CH_3	PCN-918
Empirical formula	$C_{66}H_{27}Cl_3Eu_6O_{35}$	$C_{66}H_{39}Eu_6N_3O_{35}$	$C_{69}H_{36}Eu_6O_{35}$	$C_{88}H_{50}Eu_9O_{45}$	$C_{31.5}H_{16.5}Eu_{2.25}O_{12.25}$
Formula weight	2397.94	2345.71	2336.69	3194.92	932.86
Temperature/K	150(10)	150(10)	150(10)	150(10)	150(10)
Crystal system	hexagonal	hexagonal	hexagonal	tetragonal	orthorhombic
Space group	$P6_3mc$	$P6_3mc$	$P6_3mc$	$I4_1/acd$	$Pmmn$
a/Å	22.7002(3)	22.6650(4)	22.6004(4)	35.1902(2)	24.3223(18)
b/Å	22.7002(3)	22.6650(4)	22.6004(4)	35.1902(2)	23.1197(7)
c/Å	16.4298(6)	16.5599(3)	16.7522(5)	68.8354(8)	17.9026(5)
α/°	90.00	90.00	90.00	90.00	90.00
β/°	90.00	90.00	90.00	90.00	90.00
γ/°	120.00	120.00	120.00	90.00	90.00
Volume/Å^3	7332.0(3)	7367.2(3)	7410.3(3)	85242.3(14)	10067.0(9)
Z	2.00004	2.00004	2.00004	16	8
ρ_{calc} g/cm^3	1.086	1.057	1.047	0.996	1.231

μ/mm^{-1}	18.966	18.382	18.268	18.988	20.190
F(000)	2264.	2228	2216	24080	3562
Wavelength (Å)	1.54184	1.54184	1.54184	1.54184	1.54184
2Θ range for data collection/°	7.01 to 140.71	6.98 to 133.07	6.94 to 141.32	6.81 to 133.2	7.22 to 134.08
Completeness	99.7%	99.9%	99.9%	99.6%	99.6%
Reflections collected	7689	10042	17726	63513	24400
Independent reflections	3114	3500	3645	18792	9402
R_{int}	0.0329	0.0440	0.0417	0.1081	0.0724
Data	3114	3500	3645	18792	9402
Restraints	127	128	145	86	6
Parameters	218	218	219	642	435
GOF on F^2	1.054	1.002	1.046	0.991	1.024
R1 [I > 2σ(I)]	0.0354	0.0438	0.0363	0.0881	0.0698
wR2 [I > 2σ(I)]	0.0973	0.1074	0.0992	0.2239	0.1791
R1 (all data)	0.0431	0.0570	0.0435	0.1445	0.1229
wR2 (all data)	0.1018	0.1161	0.1048	0.2692	0.2164
Residue peak / hole (eÅ^{-3})	0.65/-1.07	2.25/-0.52	1.40/-1.10	3.29/-1.4	1.43/-1.09

S4. Computational Methods

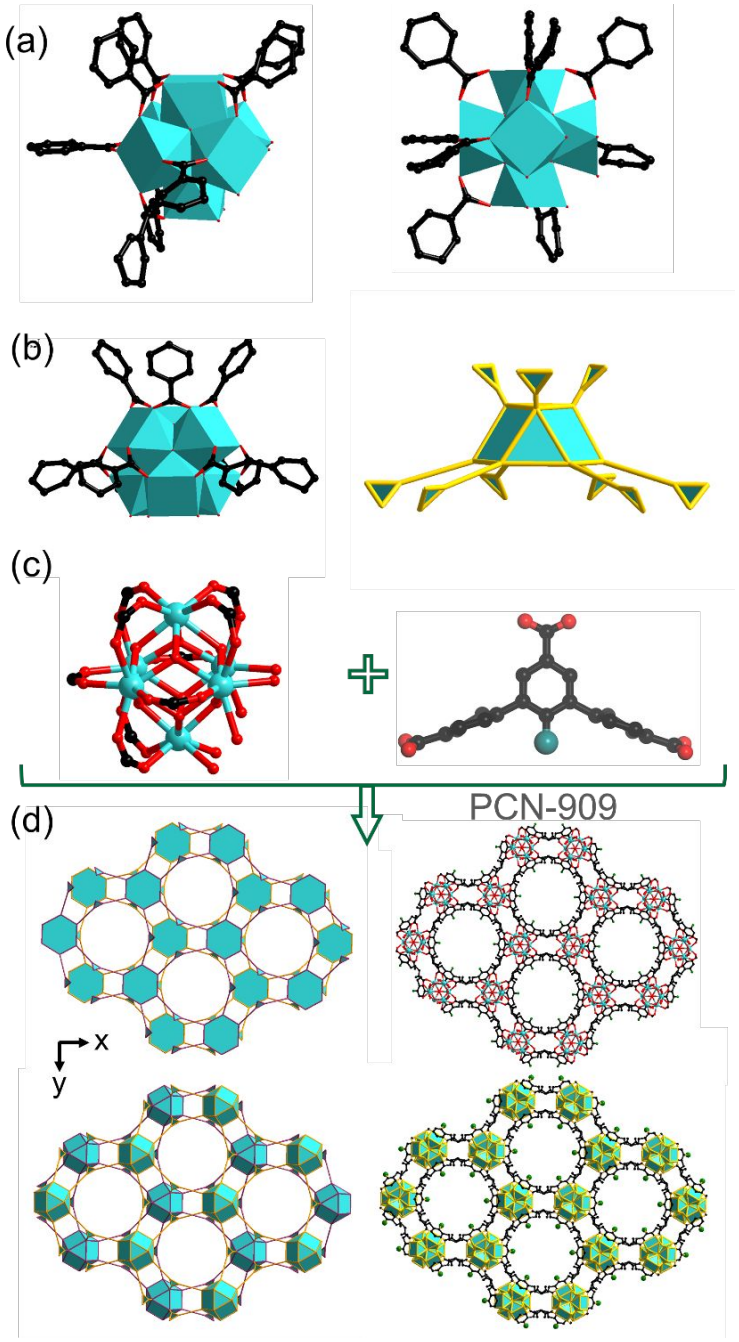

Figure S9. Structural illustration of PCN-909 and its building blocks.

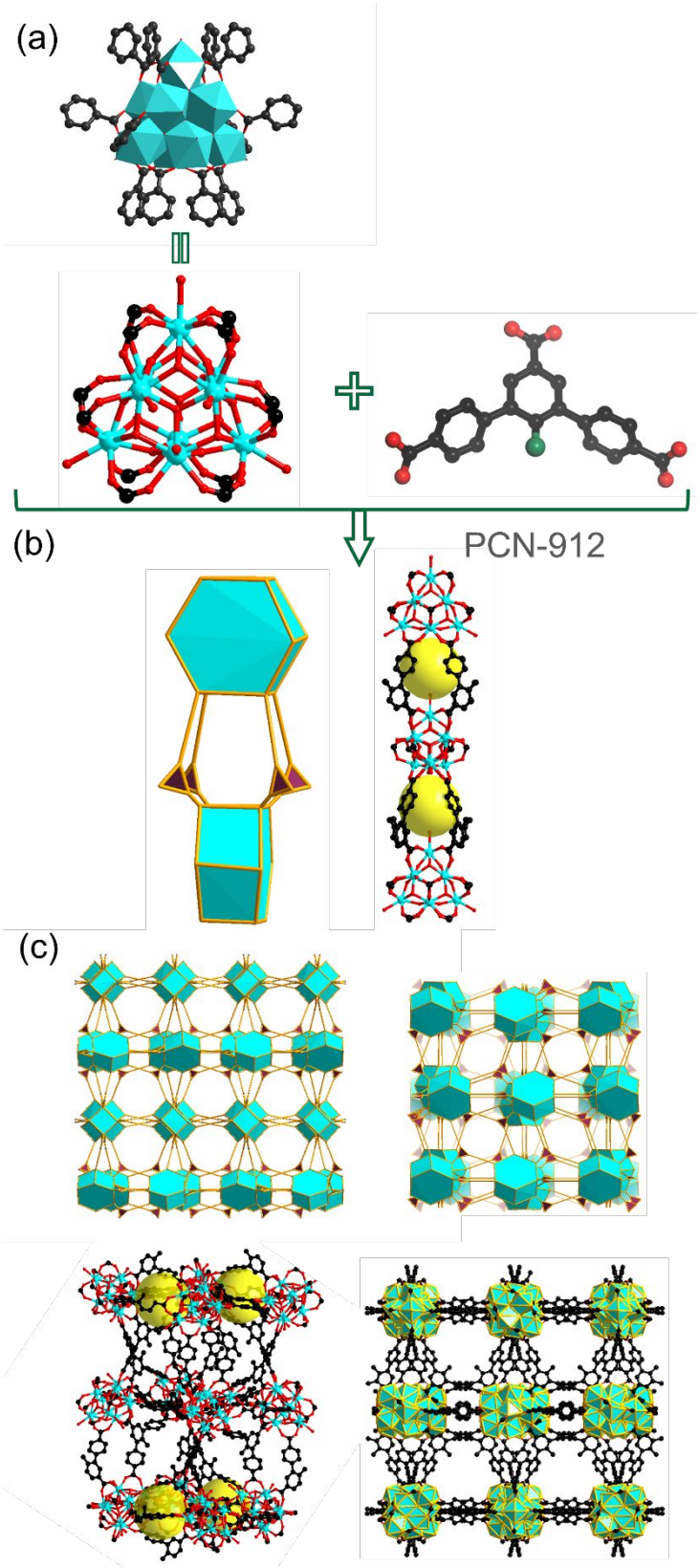

Figure S10. Structural illustration of PCN-912 and its building blocks.

Computational Methods. To interpret the relationship between linker sterics and the resulting topology, a density functional theory (DFT) study was performed by using DMol3 module of Material Studio program package.[3] The generalized gradient approximation (GGA) of the Perdew, Burke, Ernzerhof (PBE) functional and DNP 3.5 basis were employed for all calculations.[4] To simulate the states of the linkers in PCN-909, 912 and 918(RE), torsions between peripheral and central phenyl rings of ligands were constrained. For comparison, the energies of a given linker fragment in different conformations were normalized by subtracting energy of its unconstrained structure. The calculated energies of linker fragments are listed in Table S2.

Table S2. Relative energies of ligands in different RE-MOFs with unit of kJ/mol.

Ligand	Energy in PCN-909	Energy in PCN-912	Energy in PCN-918
L-Cl	6.84	6.39	11.25
L-CH_3	11.55	5.62	11.07
L-NH_2	9.18	10.47	10.24
L-OCH_3	28.67	6.36	5.00
L-F	29.50	9.65	8.55
L-H	26.62	17.92	10.78

S5. Powder X-ray Diffraction

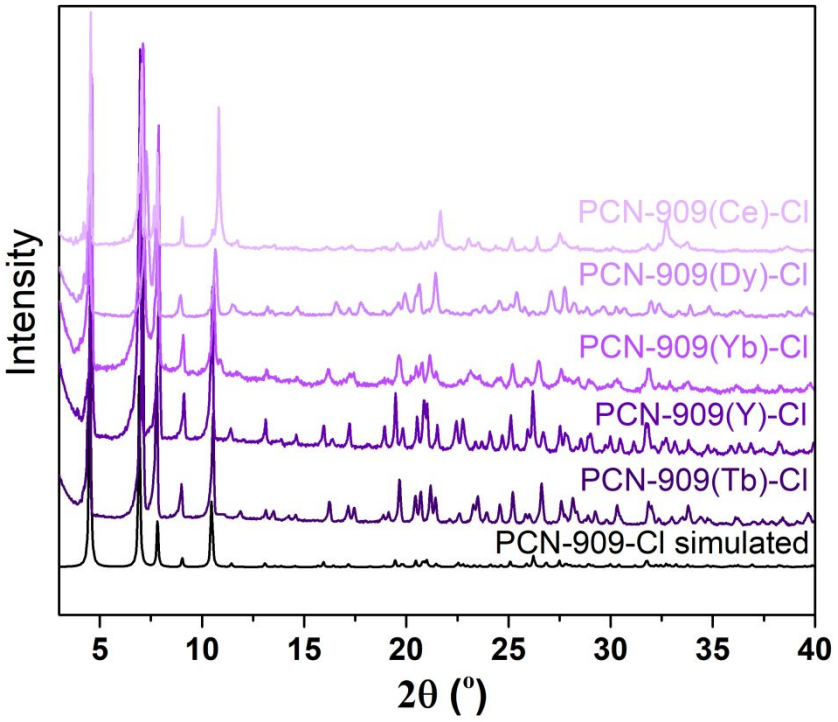

Figure S11. Powder X-ray diffraction (PXRD) patterns of PCN-909(RE)-Cl (RE = Ce, Dy, Yb, Y, Tb).

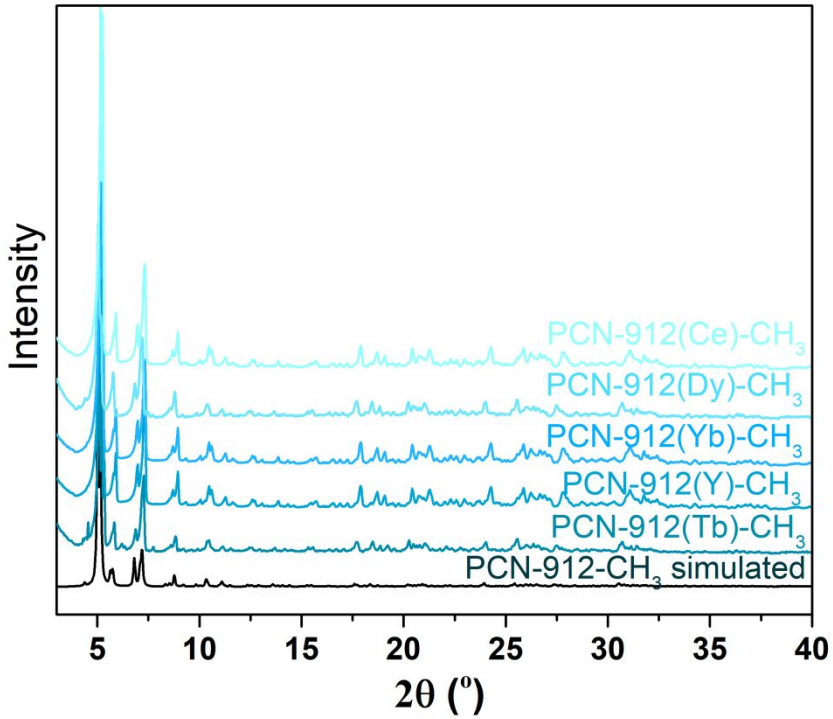

Figure S12. Powder X-ray diffraction (PXRD) patterns of mixed-linker PCN-912(RE)-CH_3 (RE = Ce, Dy, Yb, Y, Tb).

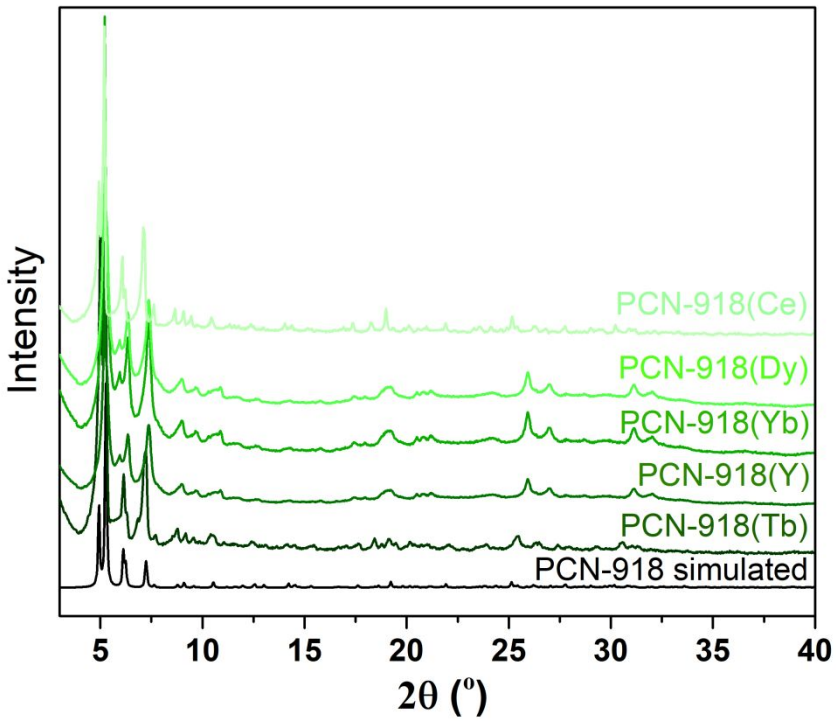

Figure S13. Powder X-ray diffraction (PXRD) patterns of PCN-918(RE) (RE = Ce, Dy, Yb, Y, Tb).

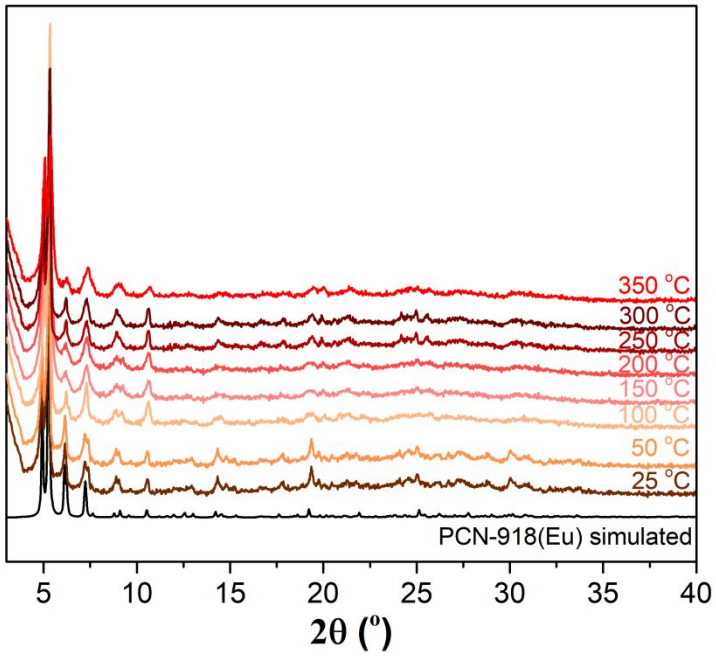

Figure S14. Variable temperature powder X-ray diffraction (PXRD) patterns of PCN-918(Eu). As indicated by the variable temperature PXRD results, the crystallinity of PCN-918(Eu) can be well-maintained up to 350 °C due to the high connectivity number (18) in the PCN-918.

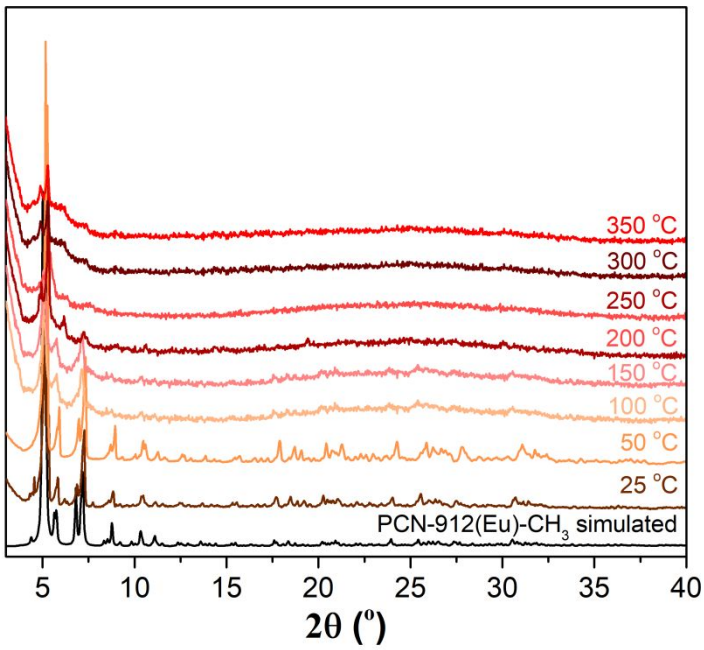

Figure S15. Variable temperature powder X-ray diffraction (PXRD) patterns of PCN-912(Eu)-CH_3. Due to the relatively low connectivity number, PCN-912 shown lower stability compared with PCN-918, as indicated by the decreasing PXRD intensity starting from around 200 °C.

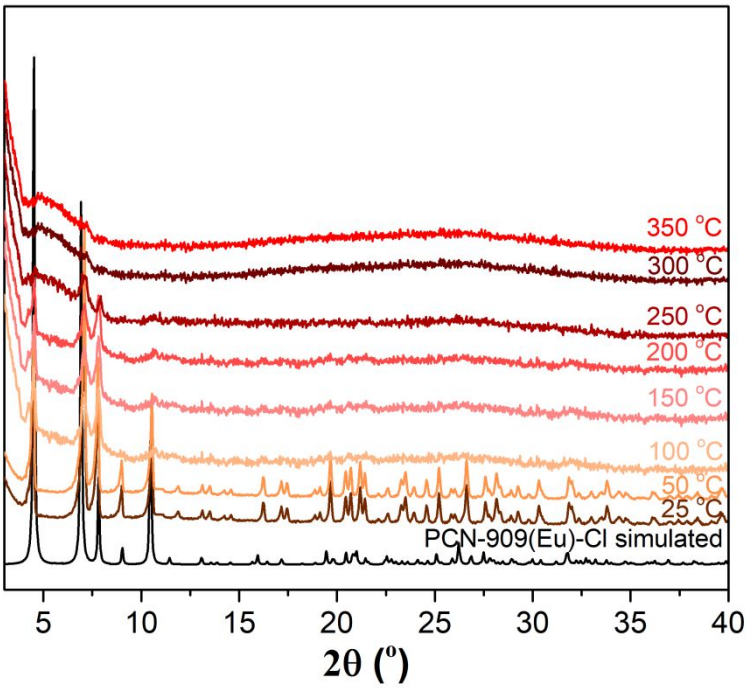

Figure S16. Variable temperature powder X-ray diffraction (PXRD) patterns of PCN-909(Eu)-Cl. Due to the relatively low connectivity number, PCN-909 shown lower stability compared with PCN-918, as indicated by the decreasing PXRD intensity starting from around 200 °C.

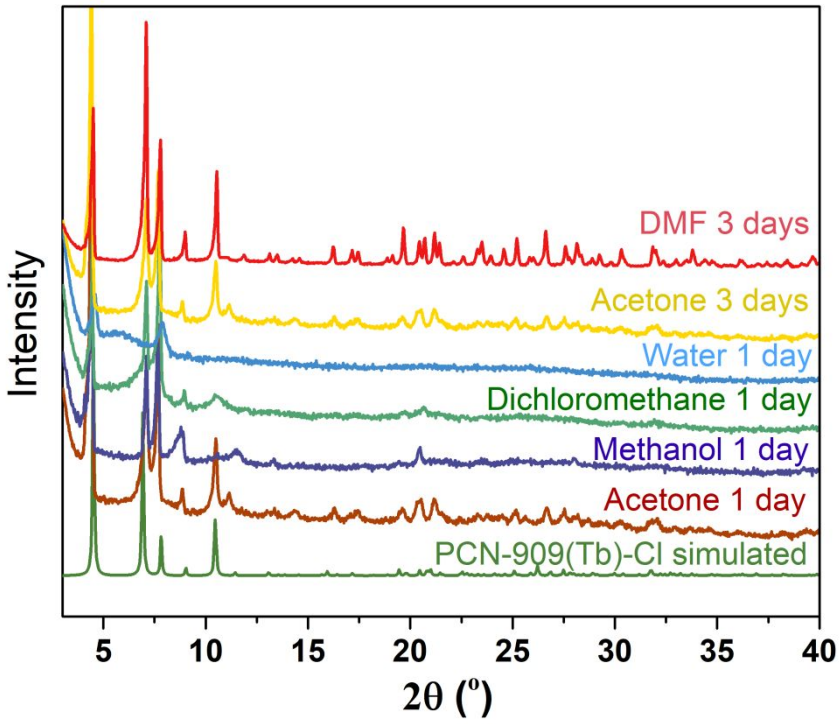

Figure S17. Powder X-ray diffraction (PXRD) patterns of PCN-909(Tb)-Cl showing chemical stability in various solvents.

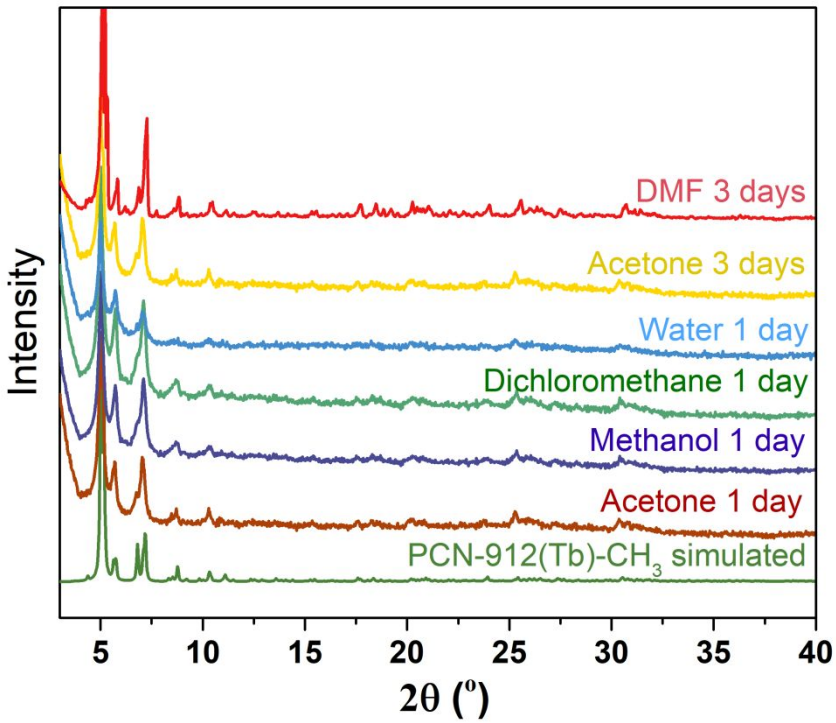

Figure S18. Powder X-ray diffraction (PXRD) patterns of PCN-912(Tb)-CH_3 showing chemical stability in various solvents.

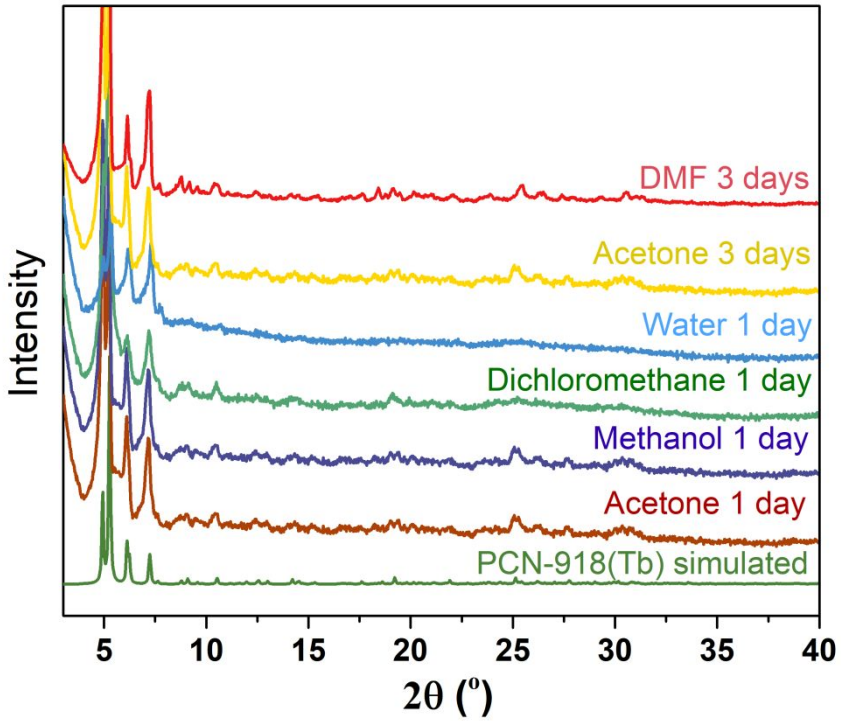

Figure S19. Powder X-ray diffraction (PXRD) patterns of mixed-linker PCN-918(Tb) showing chemical stability in various solvents.

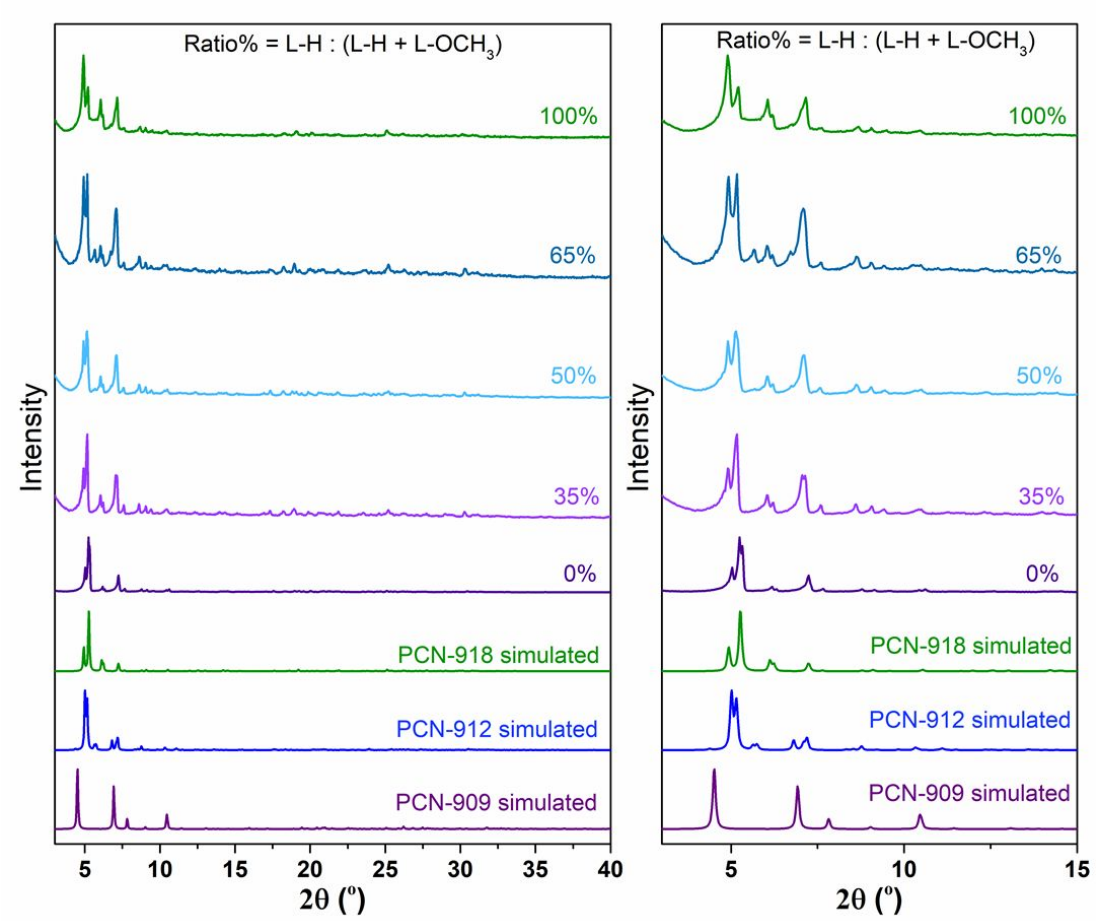

Figure S20. Powder X-ray diffraction (PXRD) patterns of mixed-linker PCN-9XX-R% (XX = 09, 12 or 18). Ratio (L-H)% = Mol (L-H) : Mol (L-H + L-OCH_3).

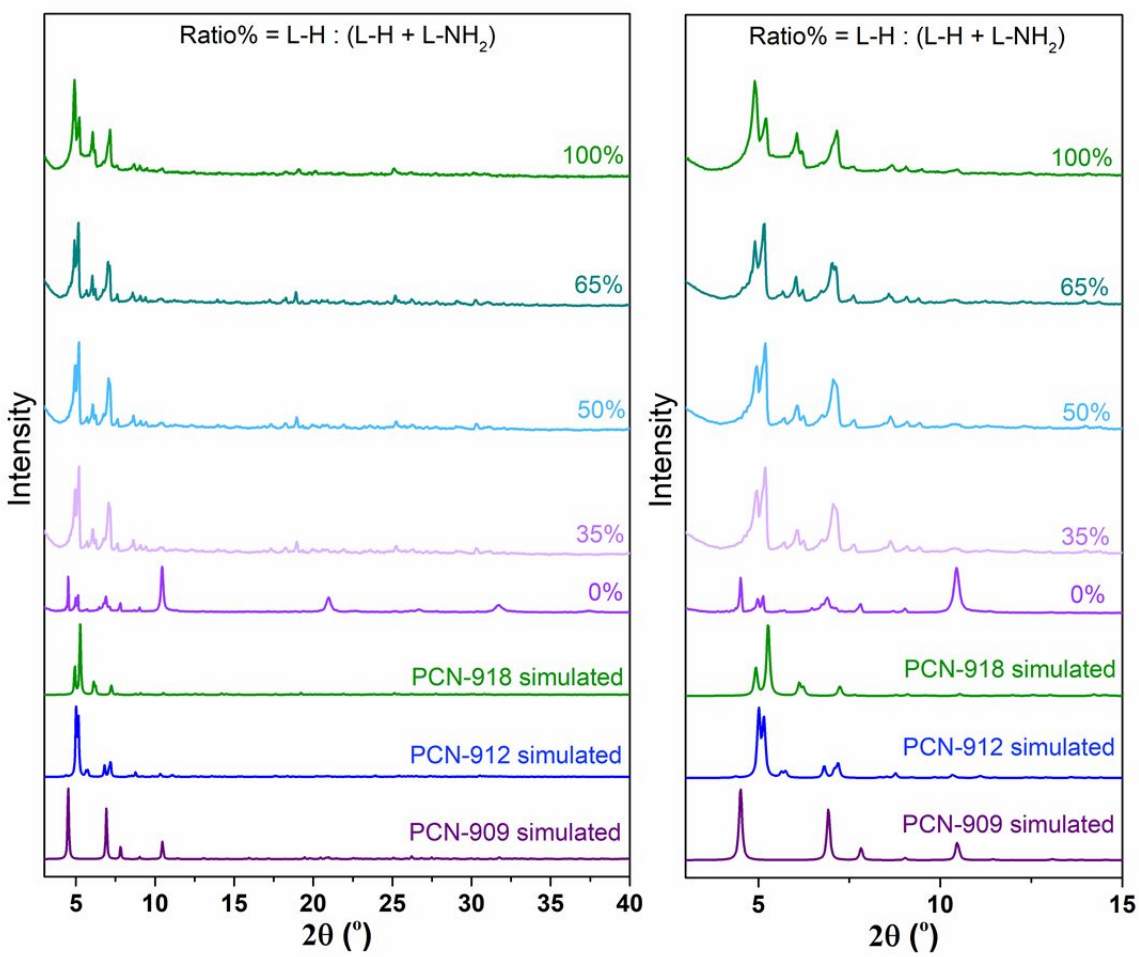

Figure S21. Powder X-ray diffraction (PXRD) patterns of mixed-linker PCN-9XX-R% (XX = 09, 12 or 18). Ratio (L-H)% = Mol (L-H) : Mol (L-H + L-NH_2).

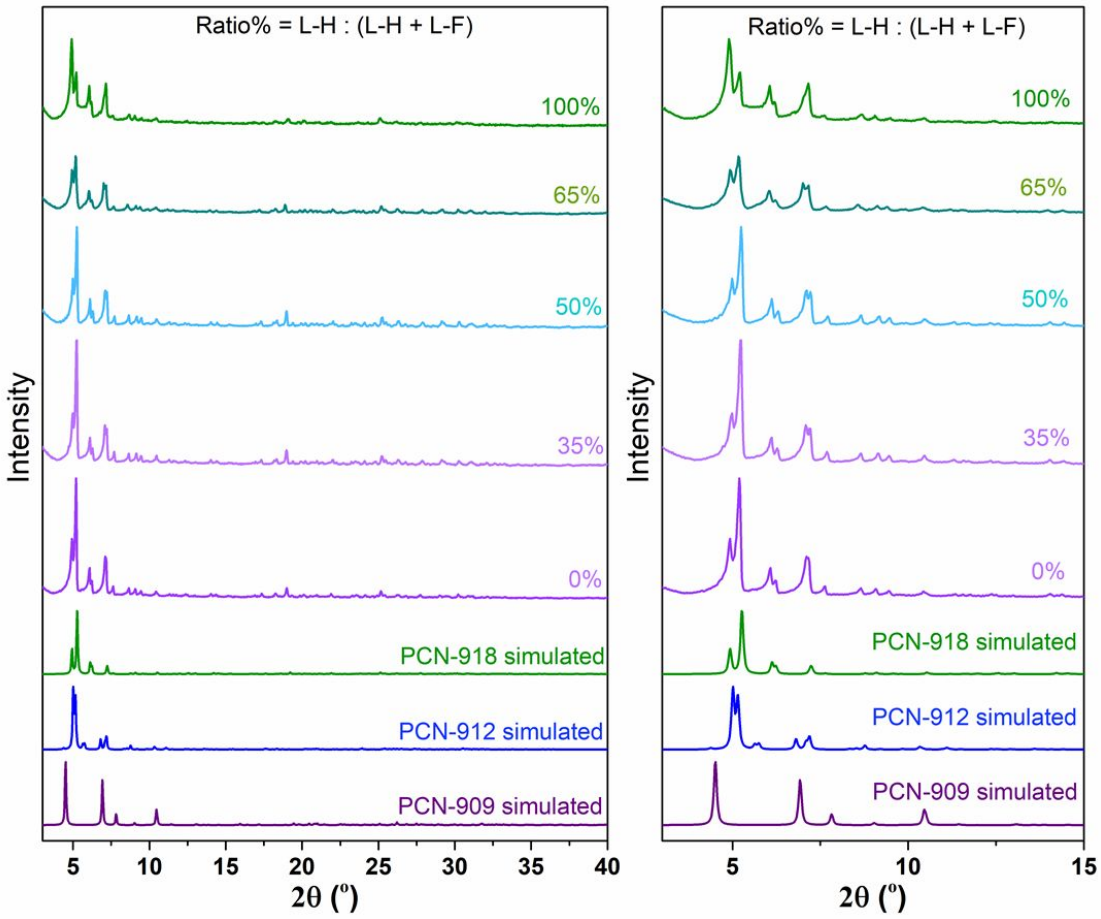

Figure S22. Powder X-ray diffraction (PXRD) patterns of mixed-linker PCN-9XX-R% (XX = 09, 12 or 18). Ratio (L-H)% = Mol (L-H) : Mol (L-H + L-F).

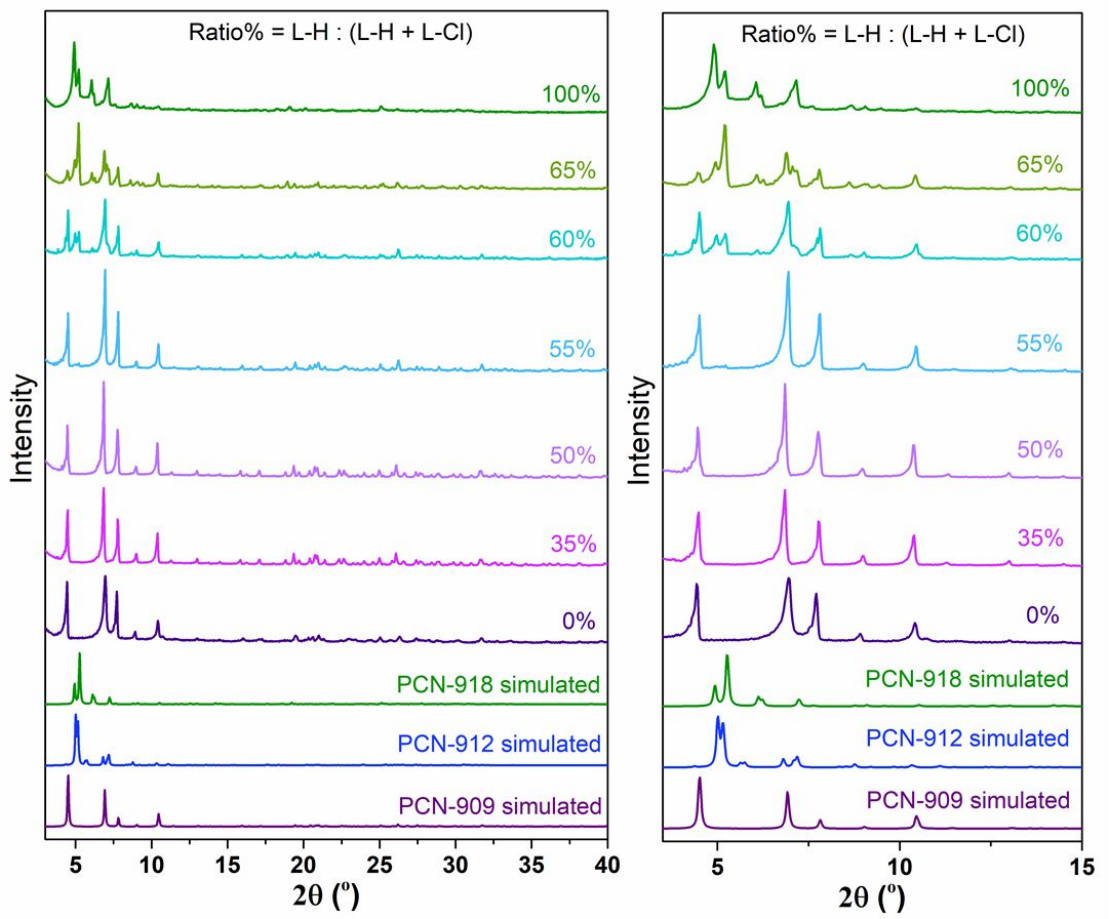

Figure S23. Powder X-ray diffraction (PXRD) patterns of mixed-linker PCN-9XX-R% (XX = 09, 12 or 18). Ratio (L-H)% = Mol (L-H) : Mol (L-H + L-Cl).

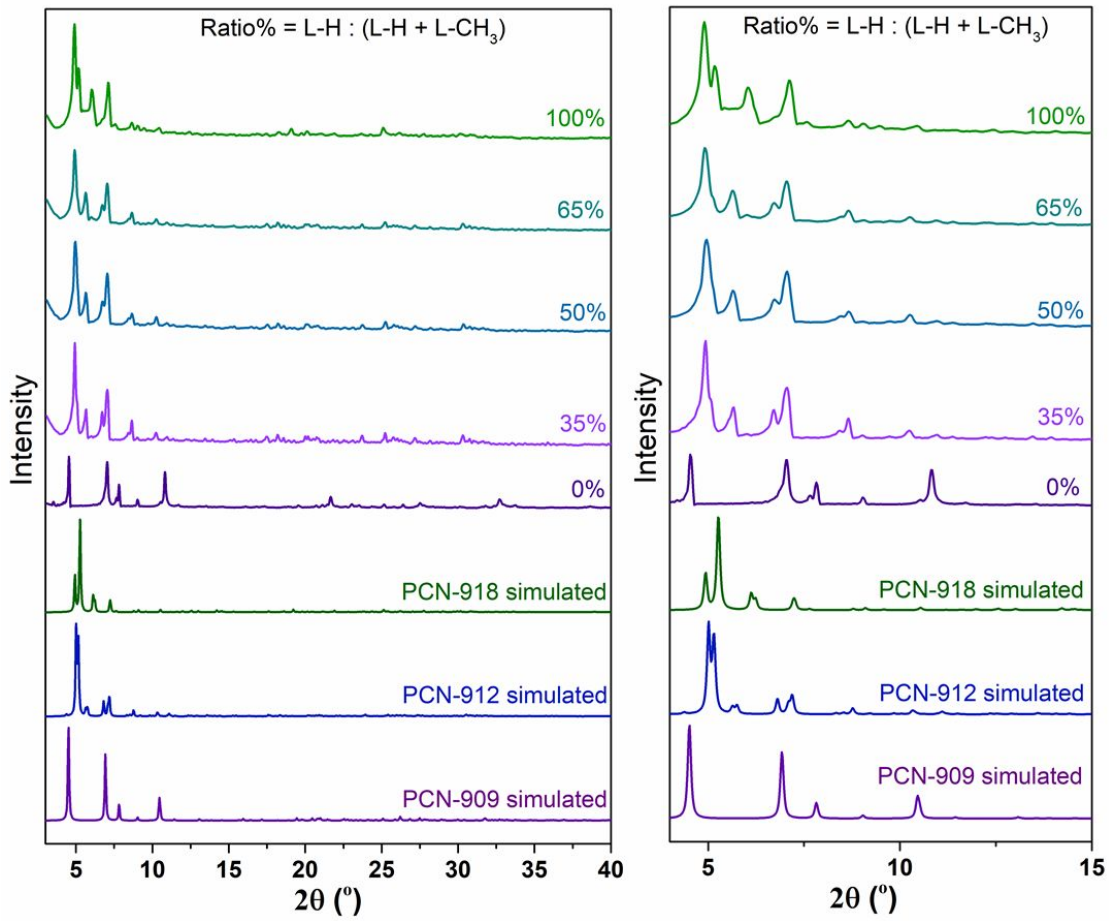

Figure S24. Powder X-ray diffraction (PXRD) patterns of mixed-linker PCN-9XX-R% (XX = 09, 12 or 18). Ratio (L-H)% = Mol (L-H) : Mol (L-H + L-CH_3).

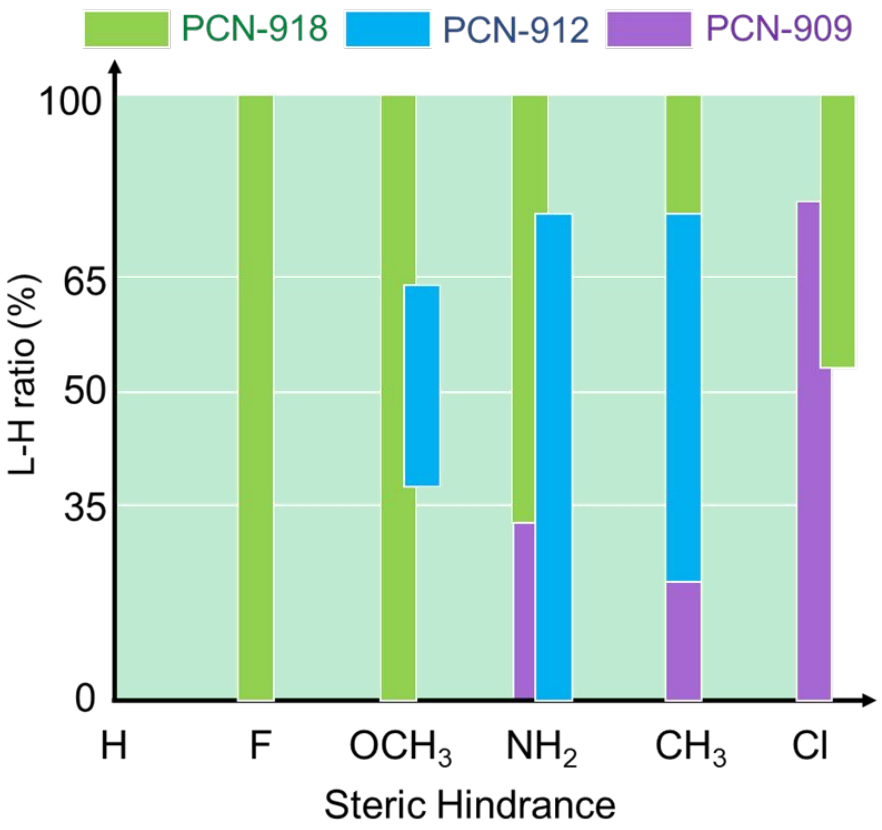

Figure S25. Phase diagram of mixed-linker PCN-909, 912 and 918.

S6. IR Spectrum

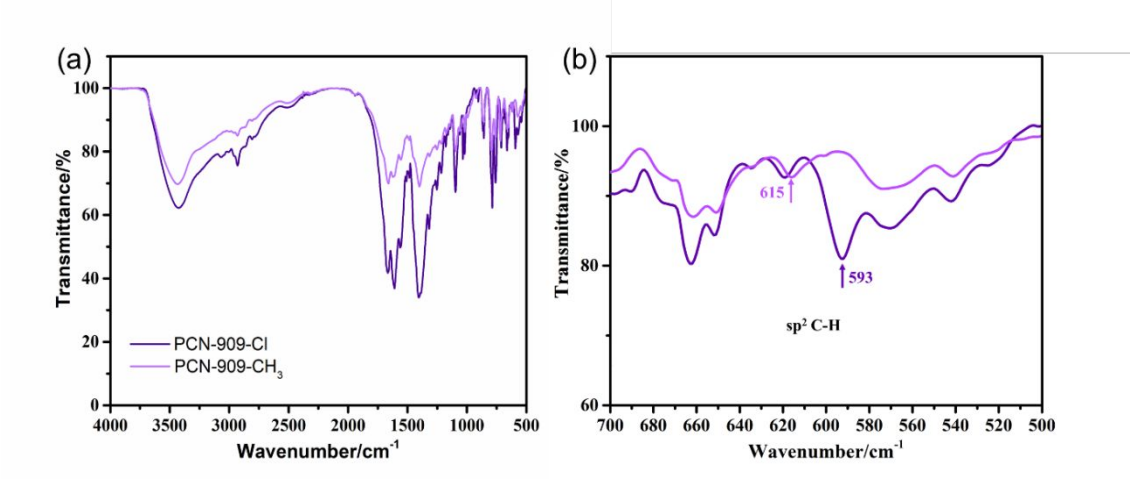

Figure S26. IR spectrum of PCN-909(Eu)-Cl and -CH_3. The introduction of functional group -Cl leads to the appearance of a new peak at 592 cm^{-1}, associated with sp^2 C-H vibration in the IR spectroscopy of PCN-909(Eu)-Cl, while the introduction of -CH_3 leads to the sp^2 C-H vibration shift to 615 cm^{-1} in the IR spectroscopy of PCN-909(Eu)-CH_3.

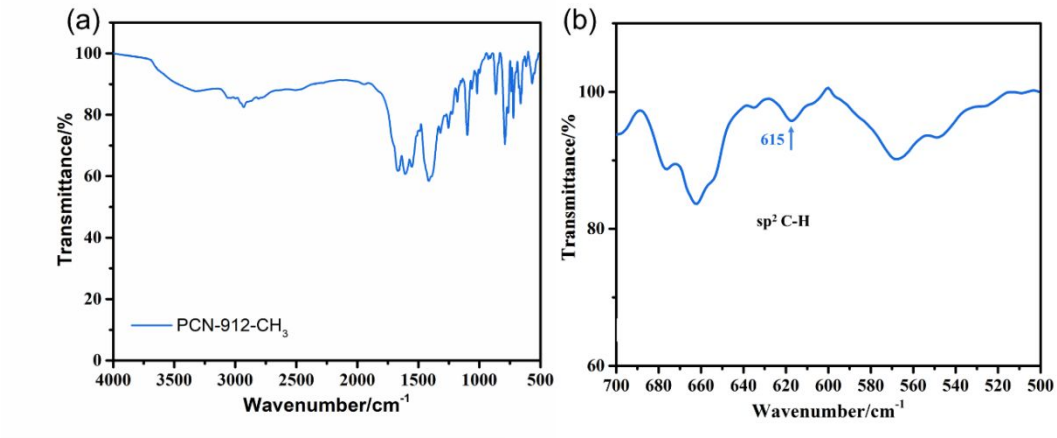

Figure S27. IR spectrum of PCN-912(Eu)-CH_3. The same signal at 615 cm^{-1} found in the IR spectroscopy of PCN-909(Eu)-CH_3 can also be accessed in the mixed-linker PCN-912(Eu)-CH_3.

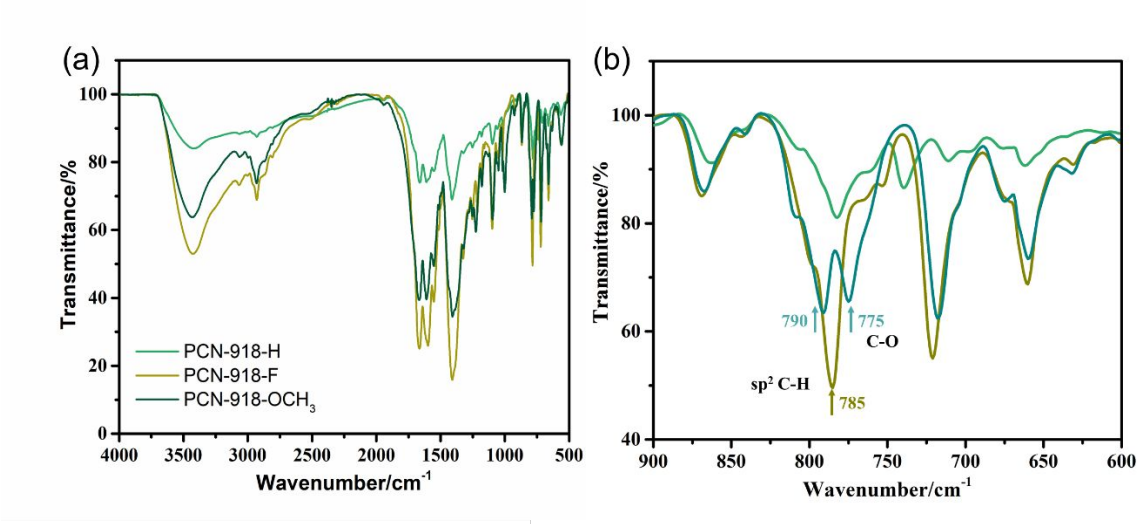

Figure S28. IR spectrum of PCN-918(Eu)-H, -F and -OCH_3. The peaks at 780 cm^{-1} are associated with the sp^2 C-H vibration modes in PCN-918(Eu)-H. The introduction of functional group -F leads to the shift of the peak to 785 cm^{-1}. The peak at 775 cm^{-1} is assigned as C-O vibration of -OCH_3 groups in the IR spectroscopy of PCN-918(Eu)-OCH_3.

S7. Gas Sorption Isotherm

Before gas sorption experiment, as-synthesized sample was washed with DMF and immersed in acetone for 3 days, during which the solvent was decanted and freshly replenished three times. The solvent was removed under vacuum at 100 °C, yielding a porous material. Gas sorption measurements were then conducted using a Micrometritics ASAP 2020 system.

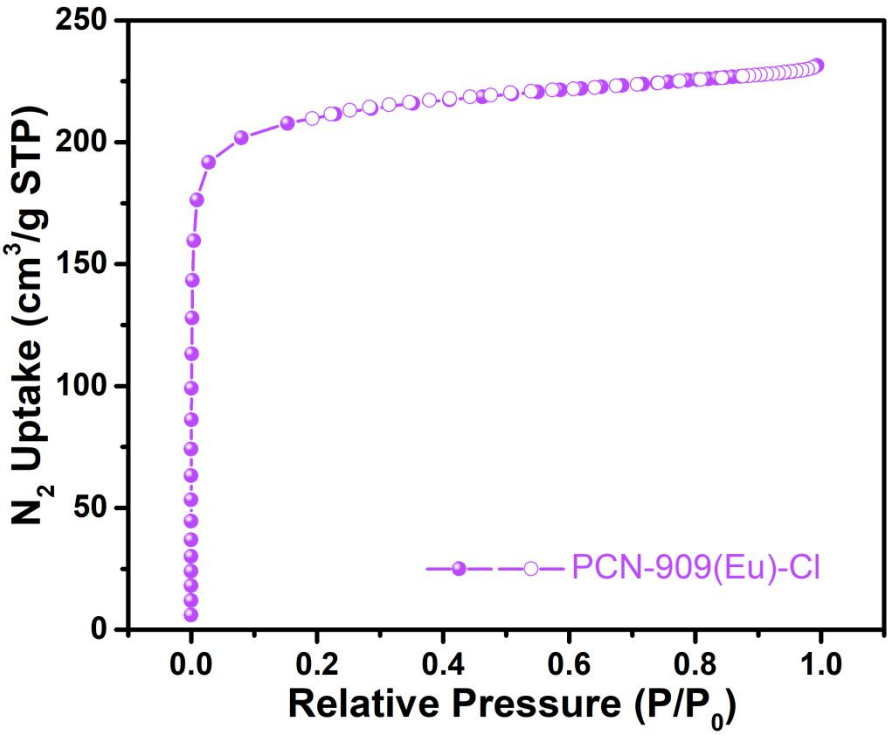

Figure S29. N_2 sorption isotherms at 77 K for PCN-909(Eu)-Cl.

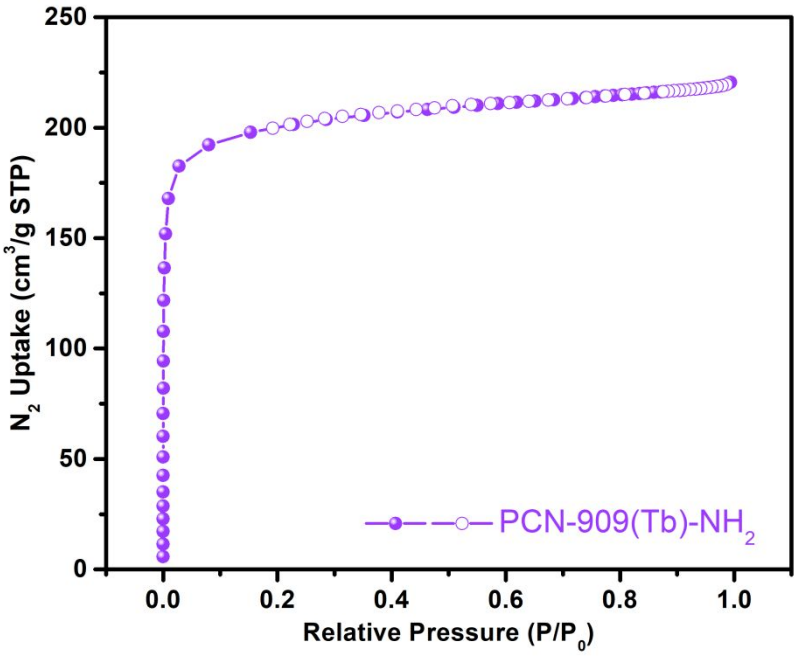

Figure S30. N_2 sorption isotherms at 77 K for PCN-909(Tb)-NH_2.

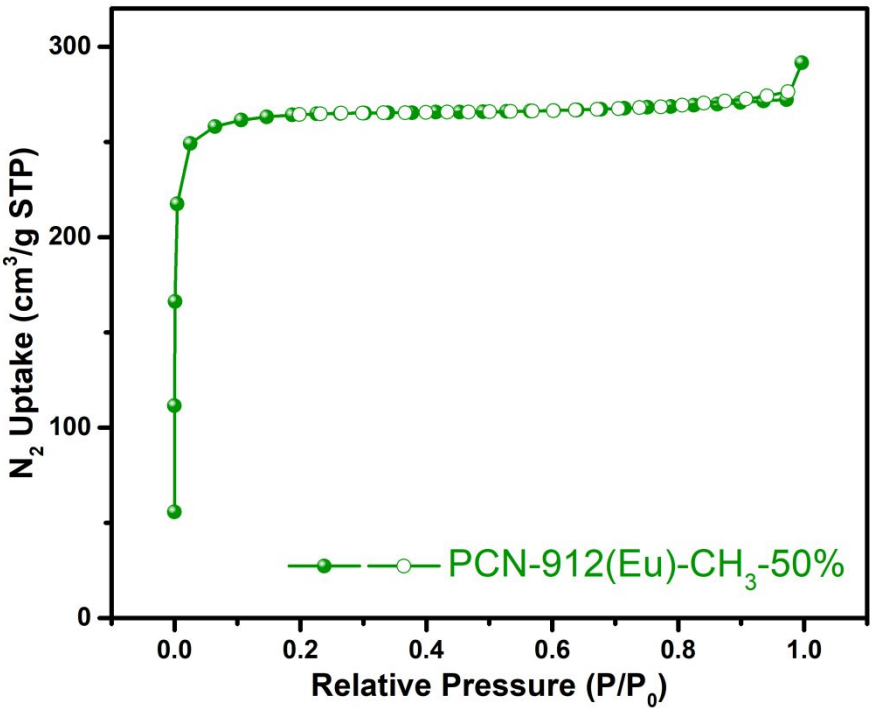

Figure S31. N_2 sorption isotherms at 77 K for PCN-912(Eu)-CH_3-50%.

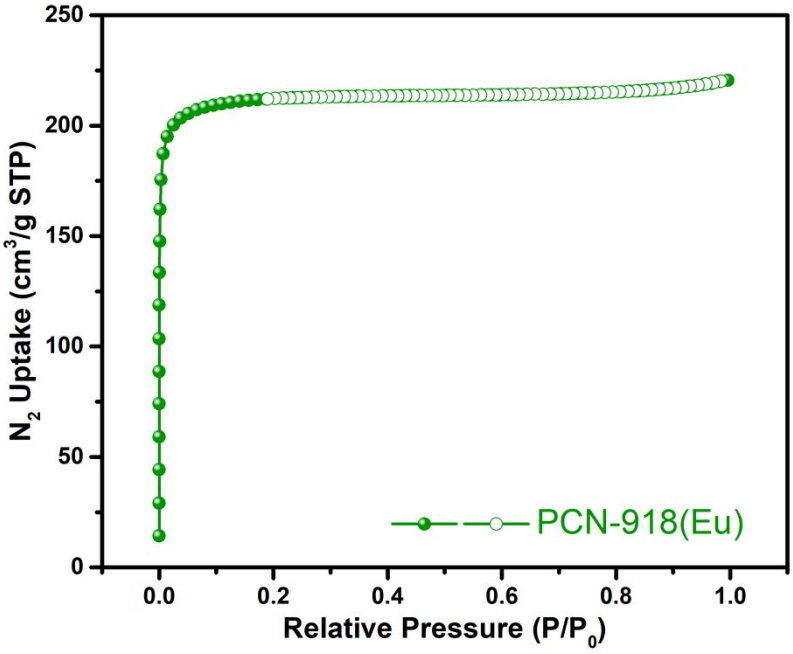

Figure S32. N_2 sorption isotherms at 77 K for PCN-918(Eu).

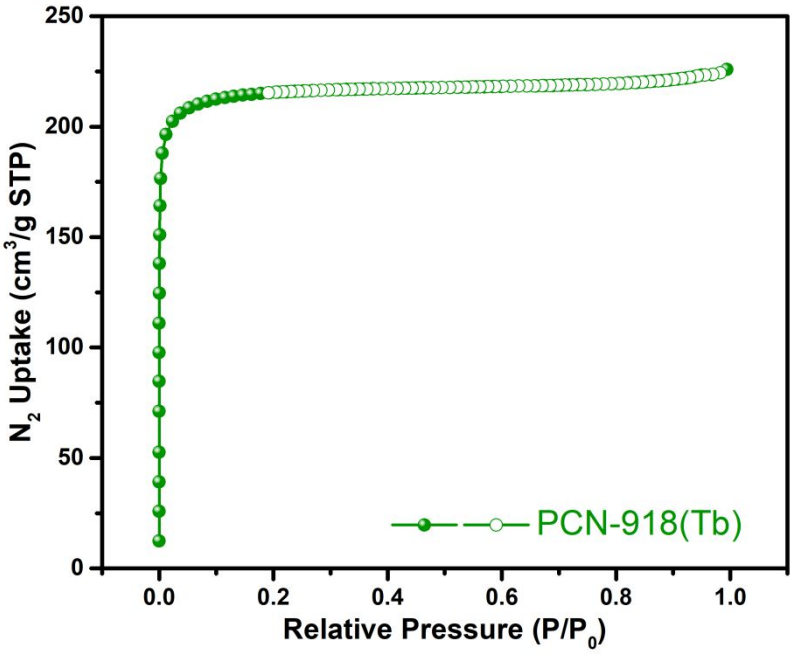

Figure S33. N_2 sorption isotherms at 77 K for PCN-918(Tb).

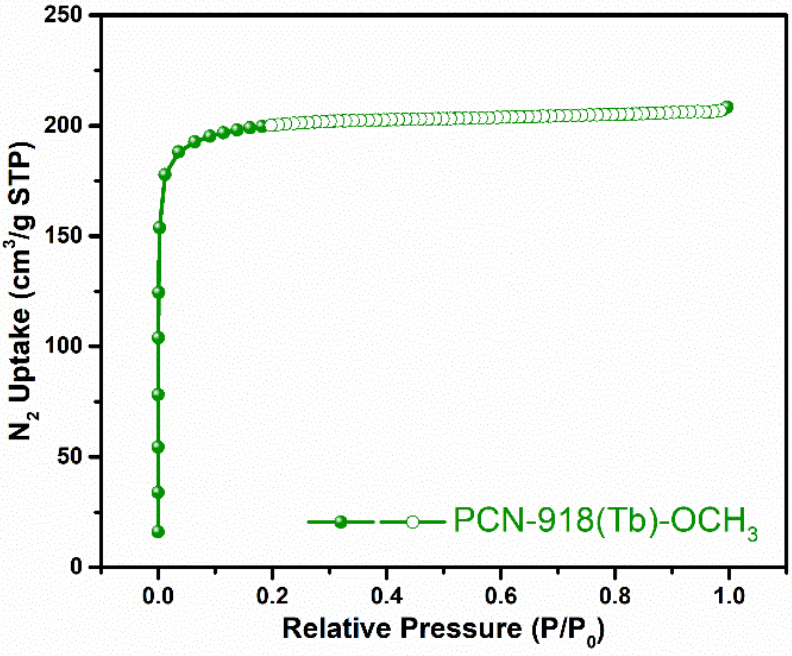

Figure S34. N_2 sorption isotherms at 77 K for PCN-918(Tb)-OCH_3.

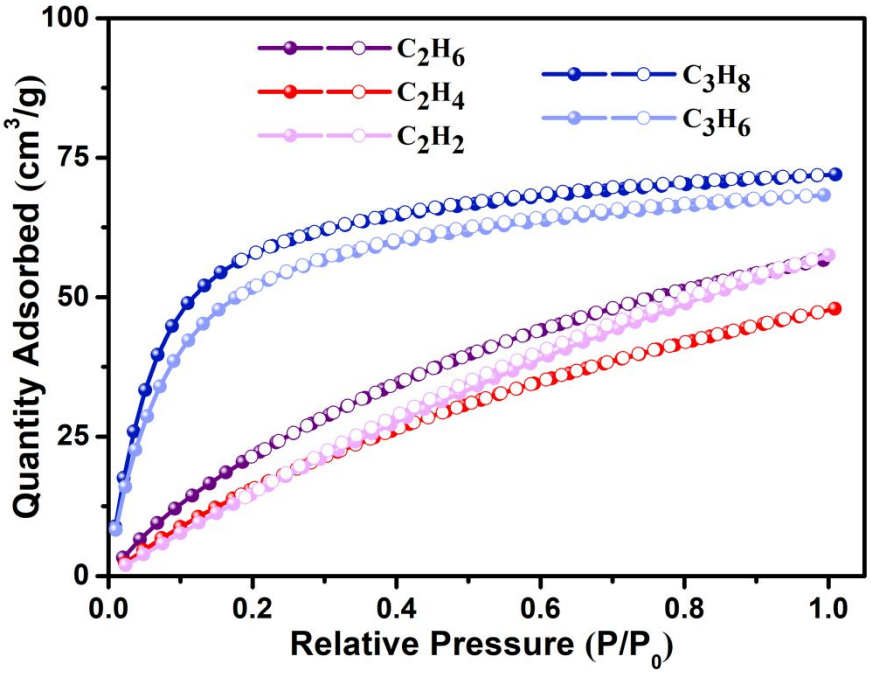

Figure S35. C_2H_6, C_2H_4, C_2H_2, C_3H_8, and C_3H_6 sorption isotherms at 273 K for PCN-909(Eu)-Cl.

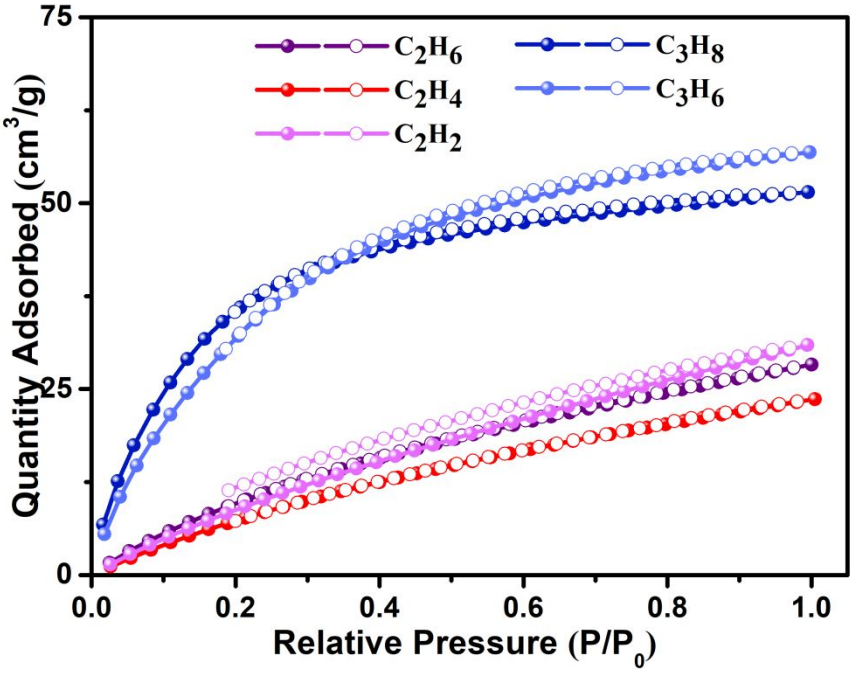

Figure S36. C_2H_6, C_2H_4, C_2H_2, C_3H_8, and C_3H_6 sorption isotherms at 298 K for PCN-909(Eu)-Cl.

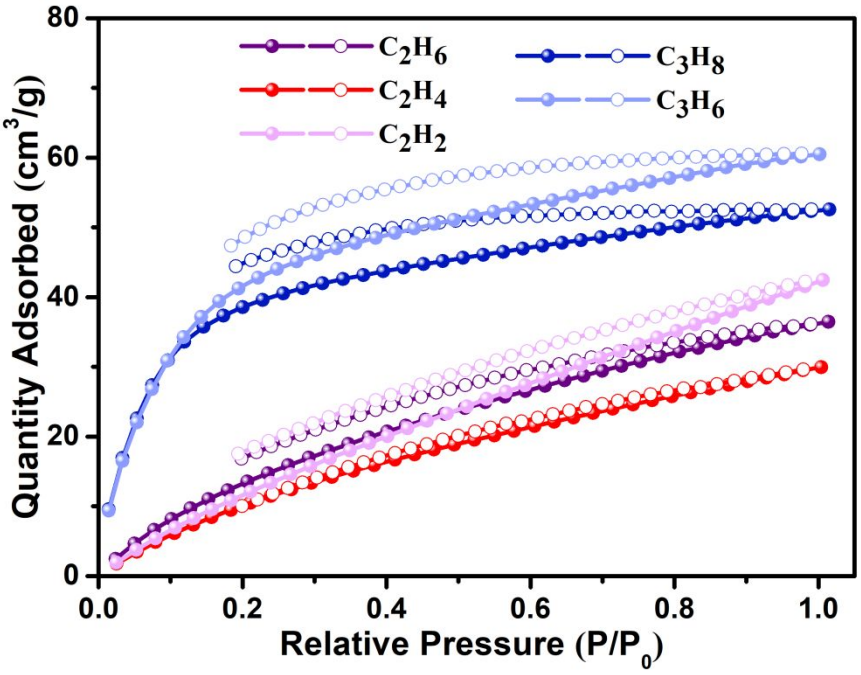

Figure S37. C_2H_6, C_2H_4, C_2H_2, C_3H_8, and C_3H_6 sorption isotherms at 273 K for PCN-909(Tb)-Cl.

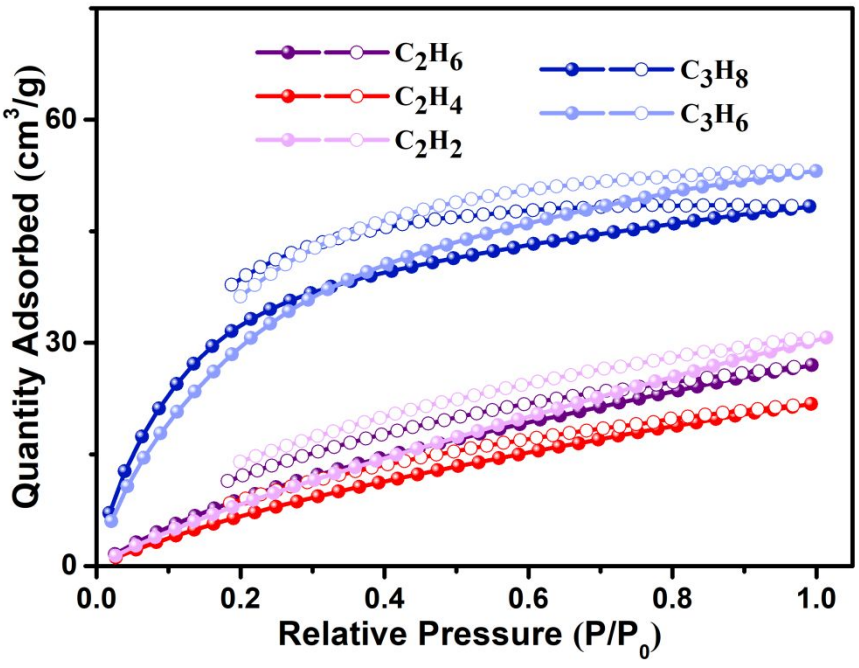

Figure S38. C_2H_6, C_2H_4, C_2H_2, C_3H_8, and C_3H_6 sorption isotherms at 298 K for PCN-909(Tb)-Cl.

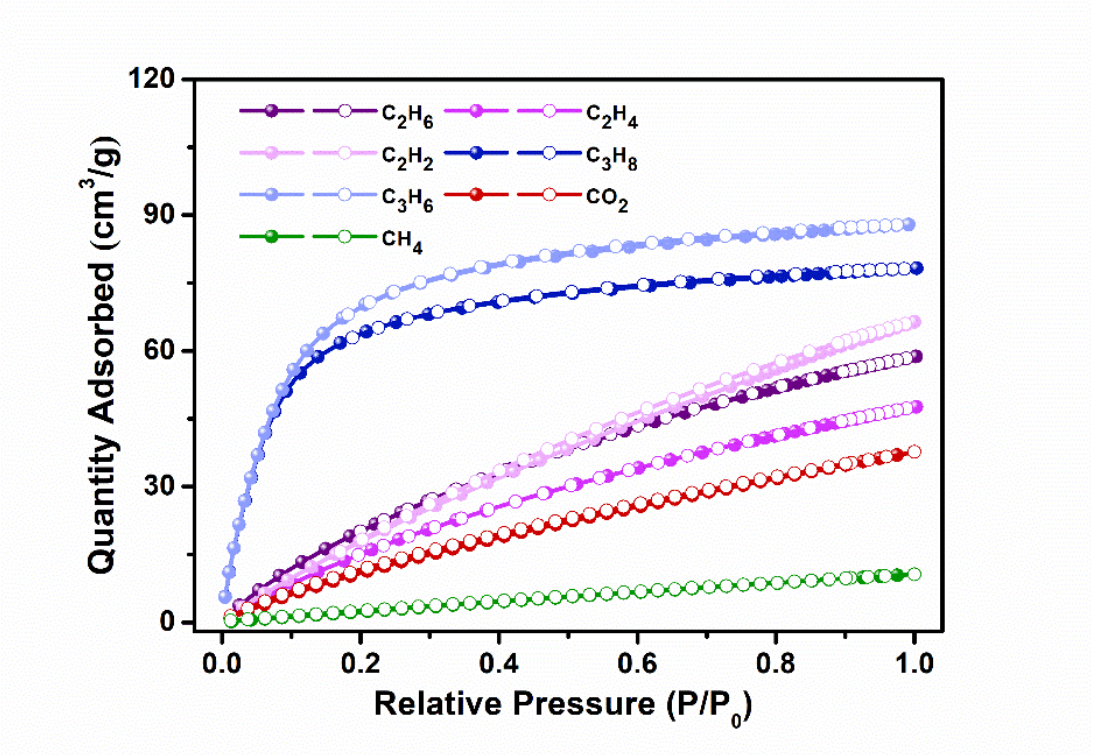

Figure S39. C_2H_6, C_2H_4, C_2H_2, C_3H_8, C_3H_6, CH_4, and CO_2 sorption isotherms at 273 K for PCN-909(Tb)-NH_2.

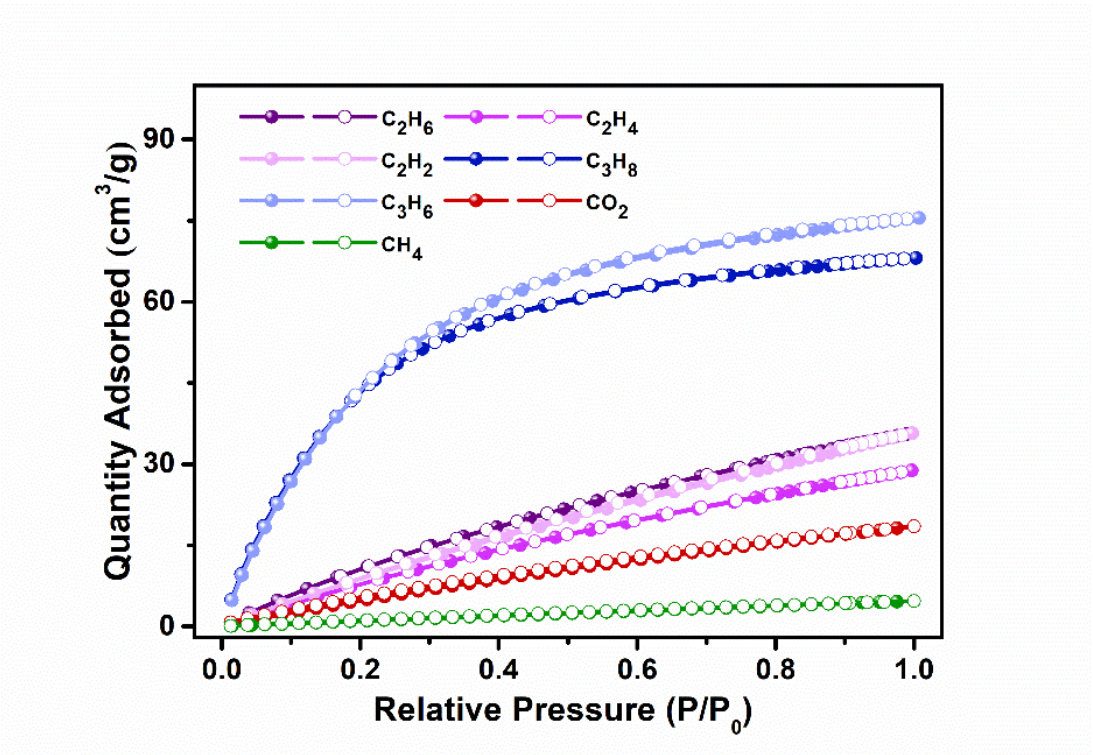

Figure S40. C_2H_6, C_2H_4, C_2H_2, C_3H_8, C_3H_6, CH_4, and CO_2 sorption isotherms at 298 K for PCN-909(Tb)-NH_2.

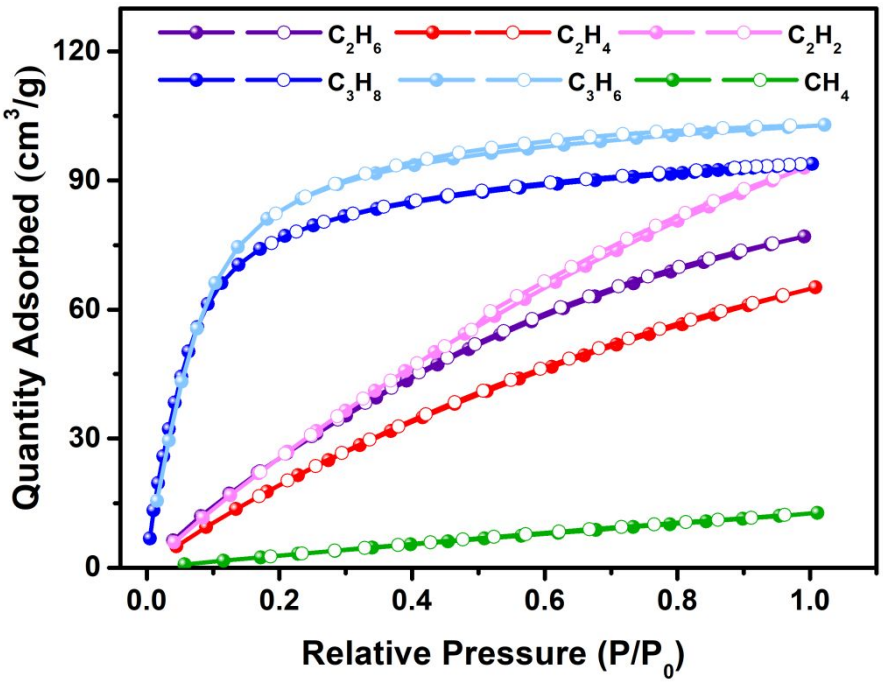

Figure S41. C_2H_6, C_2H_4, C_2H_2, C_3H_8, C_3H_6, and CH_4 sorption isotherms at 273 K for PCN-912(Tb)-CH_3.

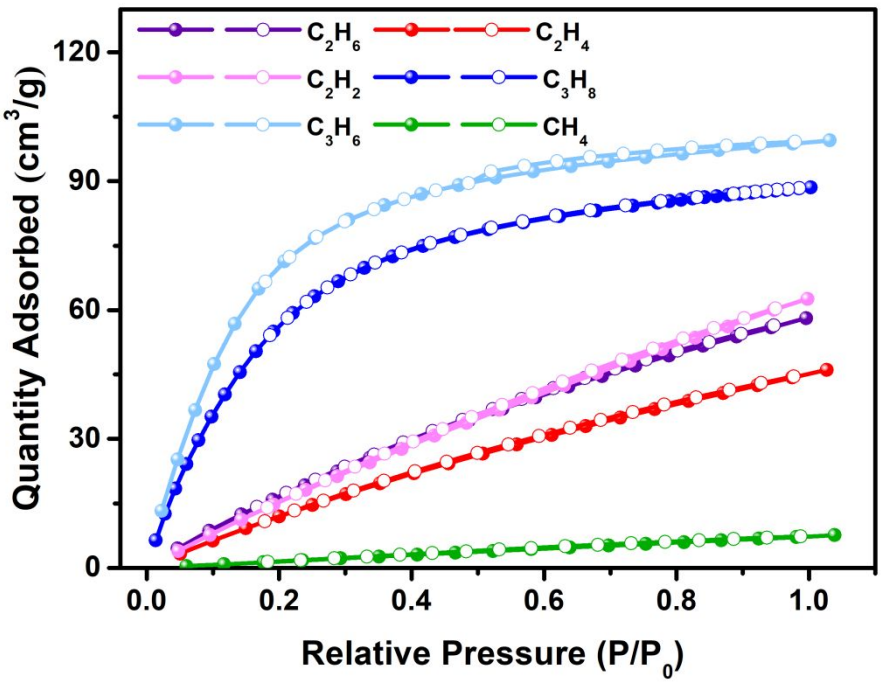

Figure S42. C_2H_6, C_2H_4, C_2H_2, C_3H_8, C_3H_6, and CH_4 sorption isotherms at 298 K for PCN-912(Tb)-CH_3.

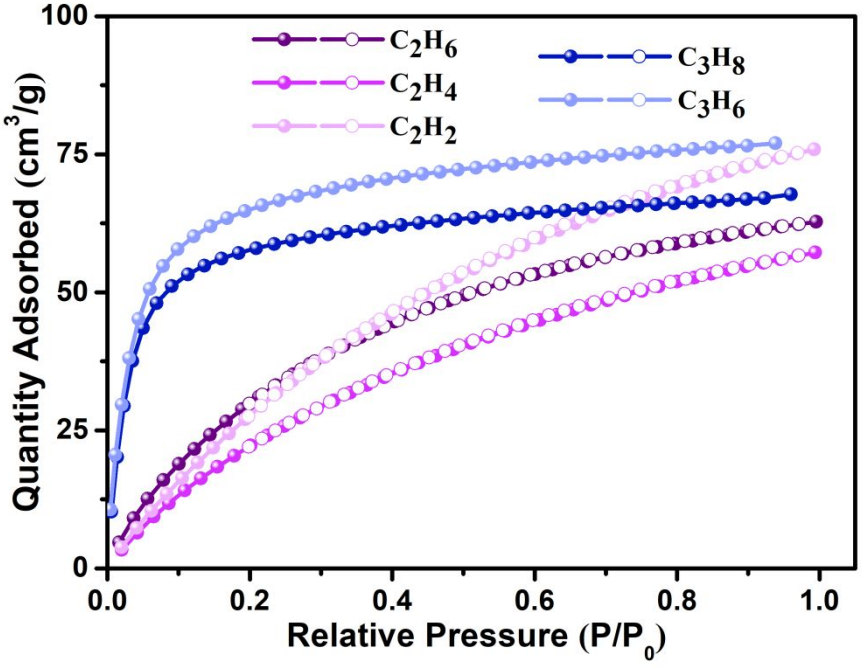

Figure S43. C_2H_6, C_2H_4, C_2H_2, C_3H_8, and C_3H_6 sorption isotherms at 273 K for PCN-918(Eu).

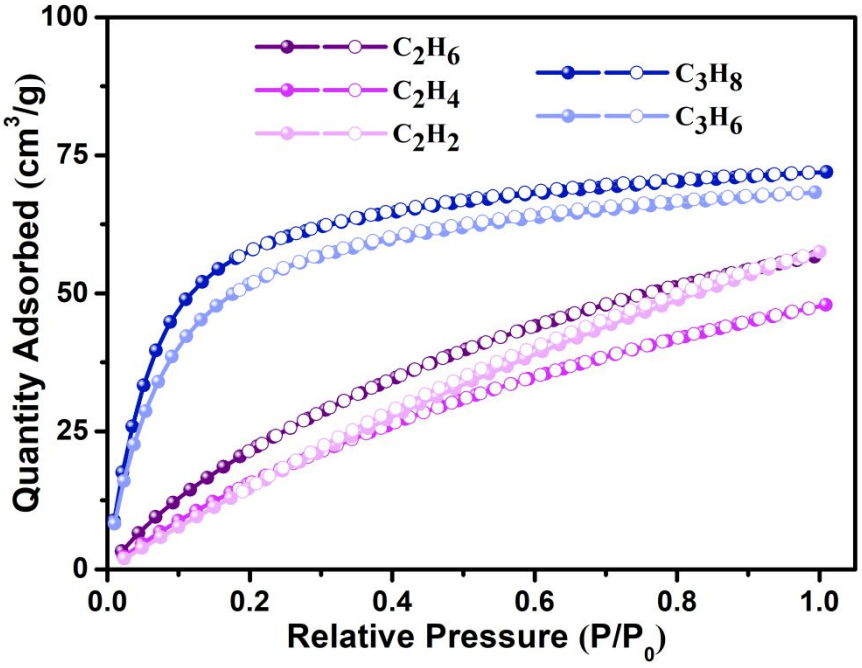

Figure S44. C_2H_6, C_2H_4, C_2H_2, C_3H_8, and C_3H_6 sorption isotherms at 298 K for PCN-918(Eu).

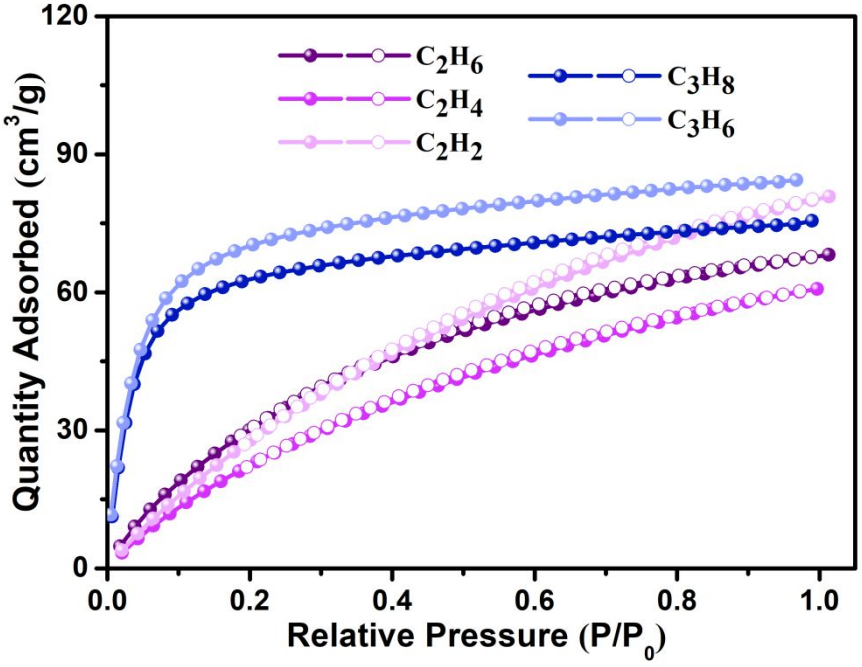

Figure S45. C_2H_6, C_2H_4, C_2H_2, C_3H_8, and C_3H_6 sorption isotherms at 273 K for PCN-918(Tb).

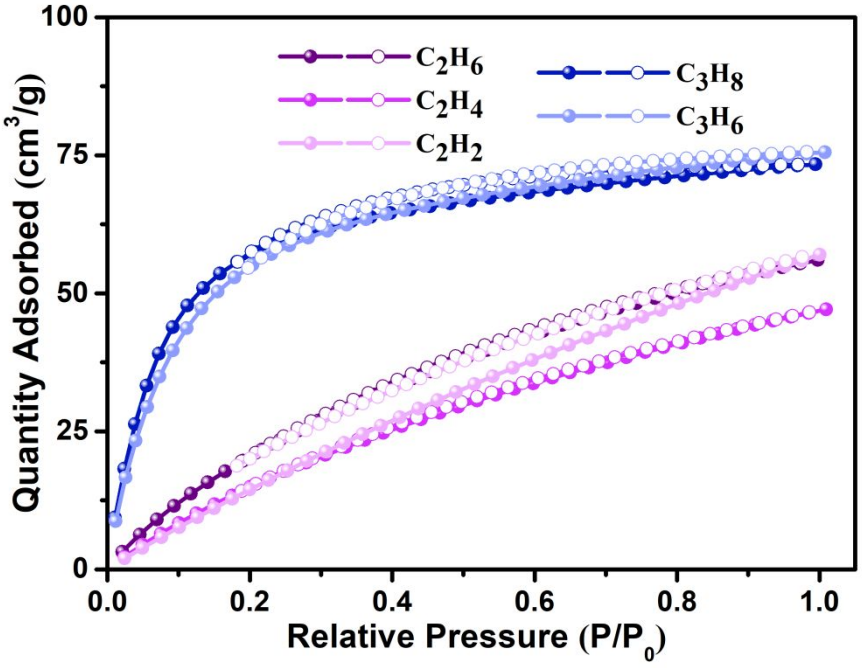

Figure S46. C_2H_6, C_2H_4, C_2H_2, C_3H_8, and C_3H_6 sorption isotherms at 298 K for PCN-918(Tb).

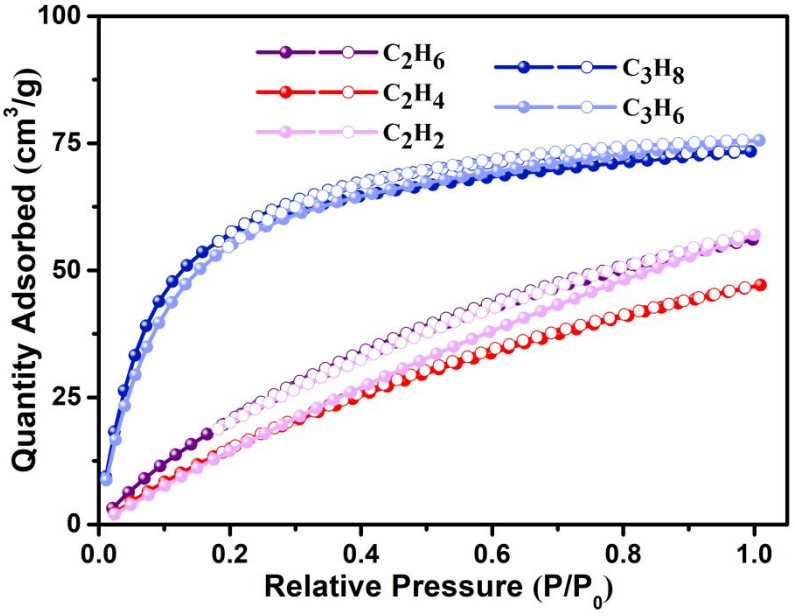

Figure S47. C_2H_6, C_2H_4, C_2H_2, C_3H_8, and C_3H_6 sorption isotherms at 273 K for PCN-918(Tb)-OCH_3.

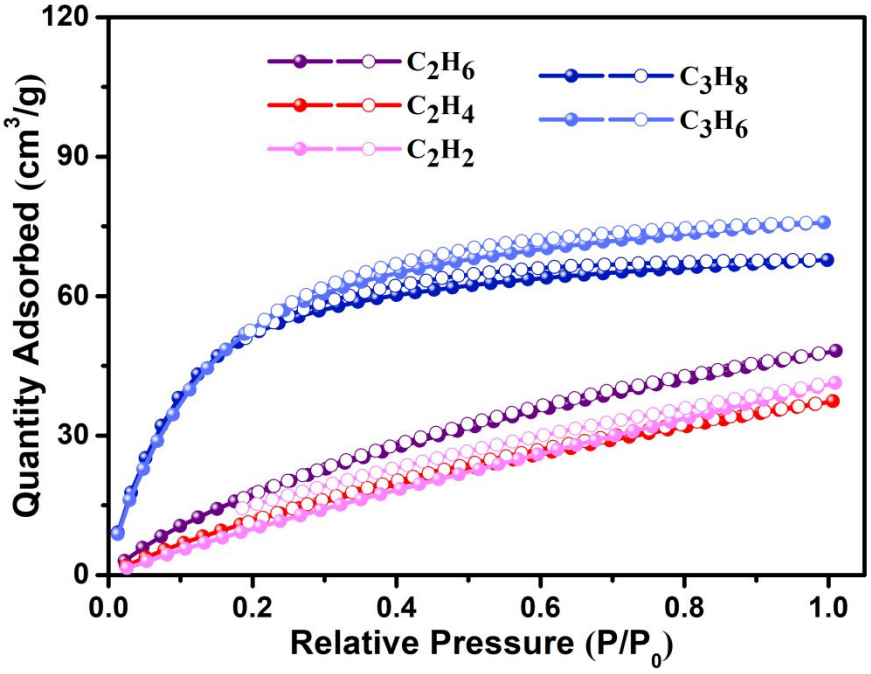

Figure S48. C_2H_6, C_2H_4, C_2H_2, C_3H_8, and C_3H_6 sorption isotherms at 298 K for PCN-918(Tb)-OCH_3.

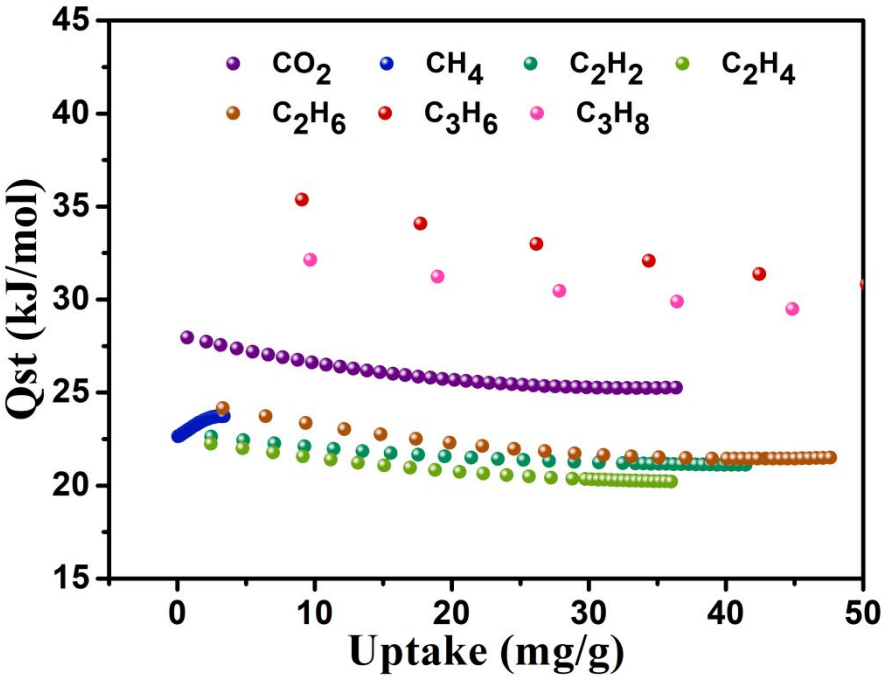

Figure S49. The gases (C_2H_6, C_2H_4, C_2H_2, C_3H_8, C_3H_6, CH_4 and CO_2) adsorption heat Q_{st} for PCN-909(Tb)-NH_2.

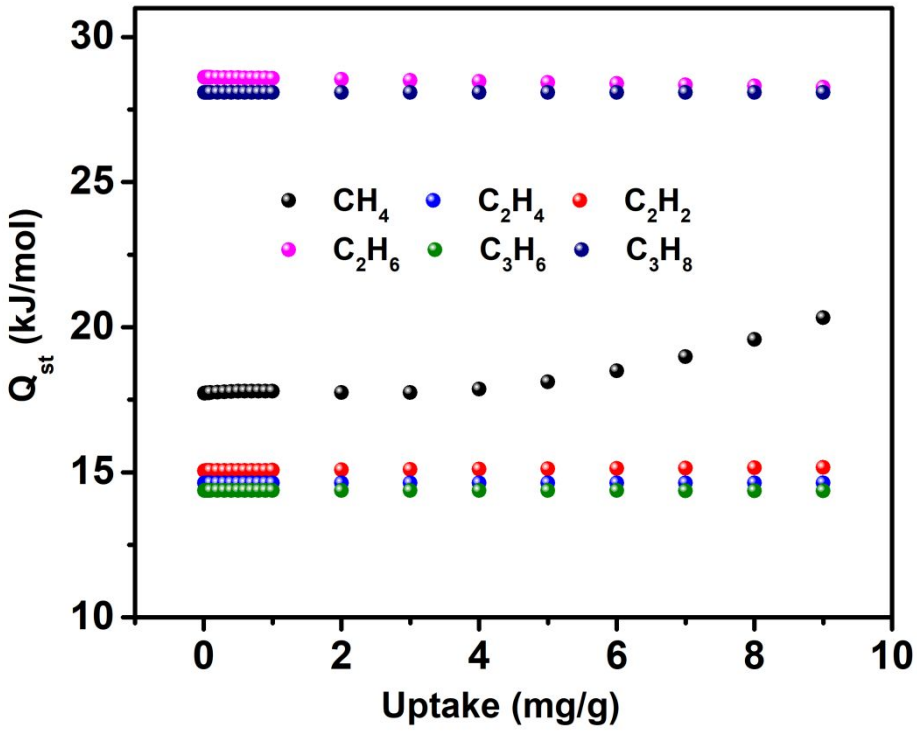

Figure S50. The gases (C_2H_6, C_2H_4, C_2H_2, C_3H_8, C_3H_6, and CH_4) adsorption heat Q_{st} for PCN-912(Tb)-CH_3.

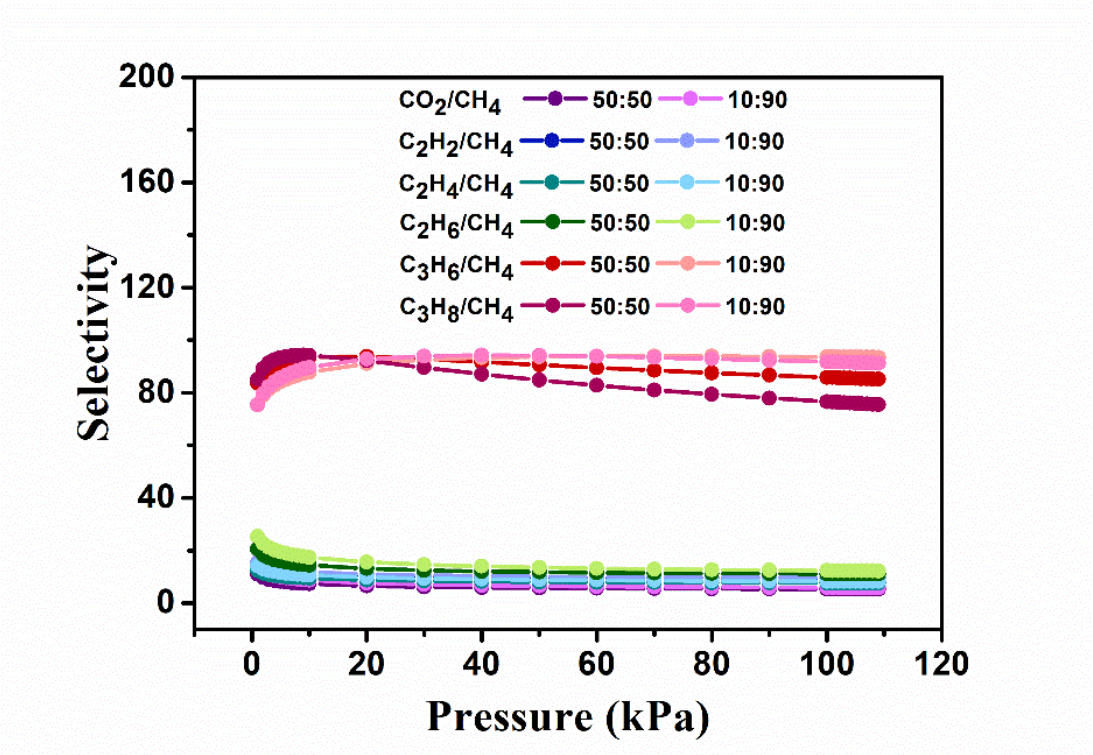

Figure S51. Adsorption selectivities of PCN-909(Tb)-NH_2 at 273 K calculated using IAST for equimolar mixtures of CO_2/CH_4, C_2H_2/CH_4, C_2H_4/CH_4, C_2H_6/CH_4, C_3H_6/CH_4 and C_3H_8/CH_4.

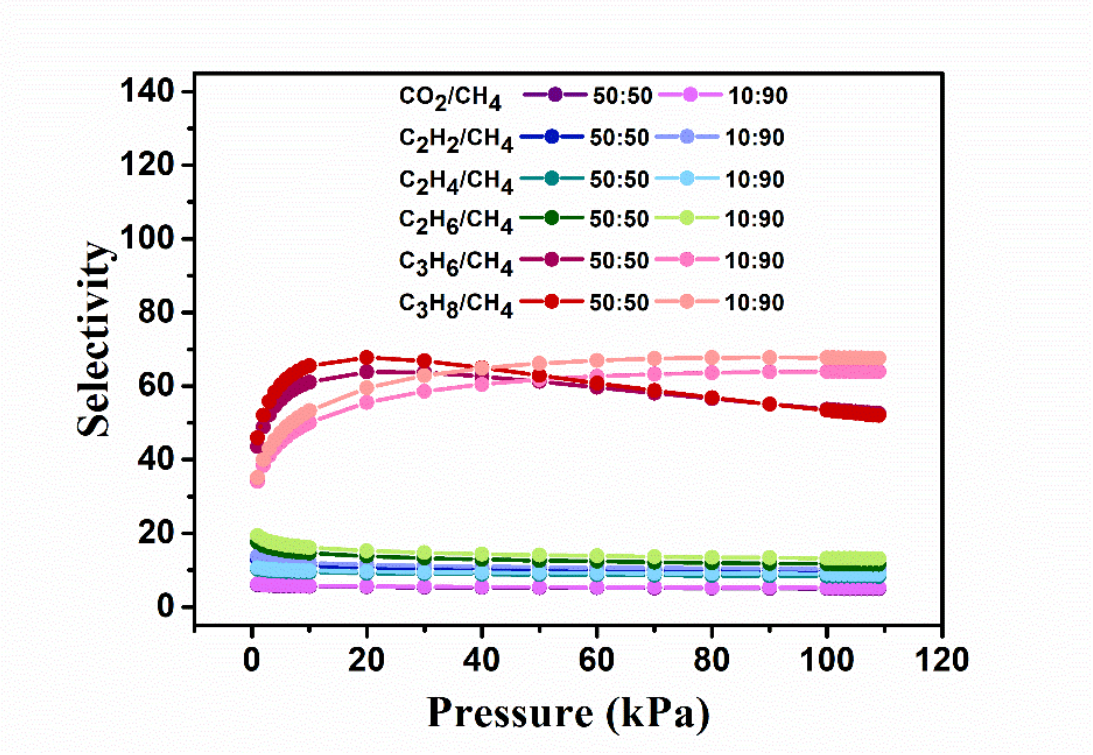

Figure S52. Adsorption selectivities of PCN-909(Tb)-NH_2 at 298 K calculated using IAST for equimolar mixtures of CO_2/CH_4, C_2H_2/CH_4, C_2H_4/CH_4, C_2H_6/CH_4, C_3H_6/CH_4 and C_3H_8/CH_4.

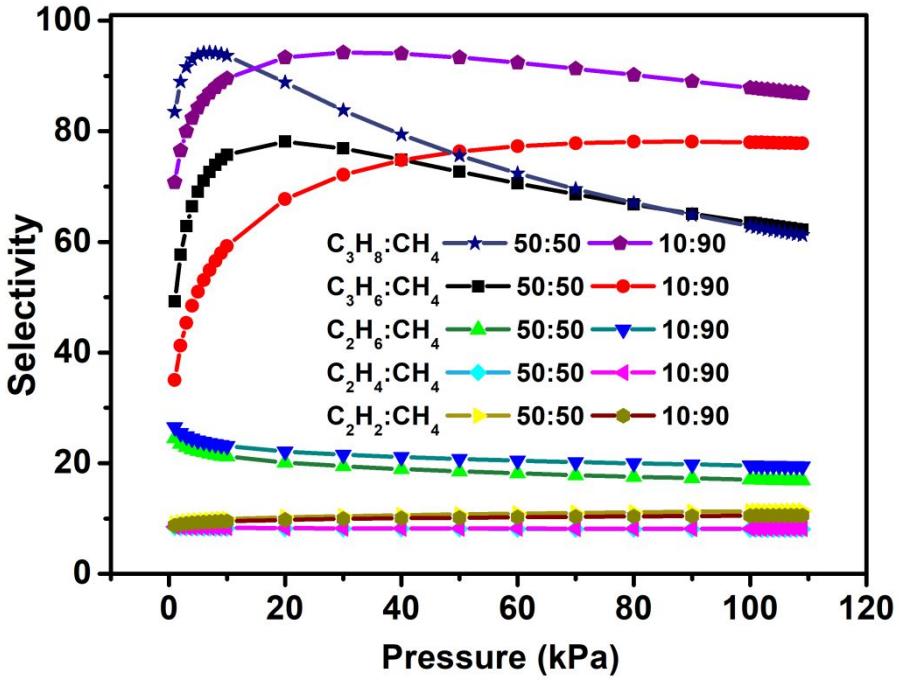

Figure S53. Adsorption selectivities of PCN-912(Tb)-CH_3 at 273 K calculated using IAST for equimolar mixtures of C_2H_2/CH_4, C_2H_4/CH_4, C_2H_6/CH_4, C_3H_6/CH_4 and C_3H_8/CH_4.

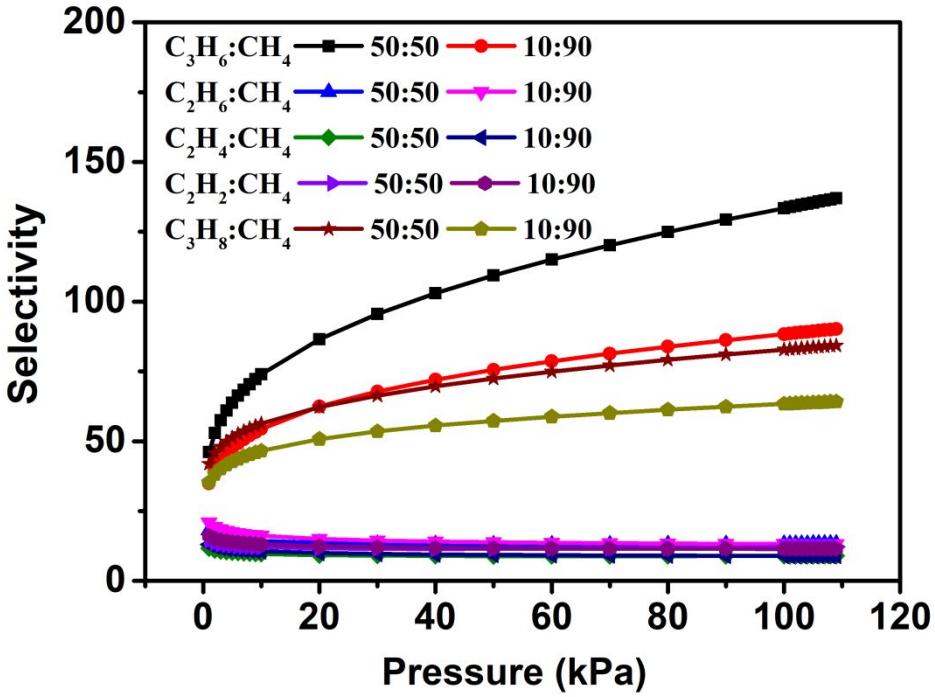

Figure S54. Adsorption selectivities of PCN-912(Tb)-CH_3 at 298 K calculated using IAST for equimolar mixtures of C_2H_2/CH_4, C_2H_4/CH_4, C_2H_6/CH_4, C_3H_6/CH_4 and C_3H_8/CH_4.

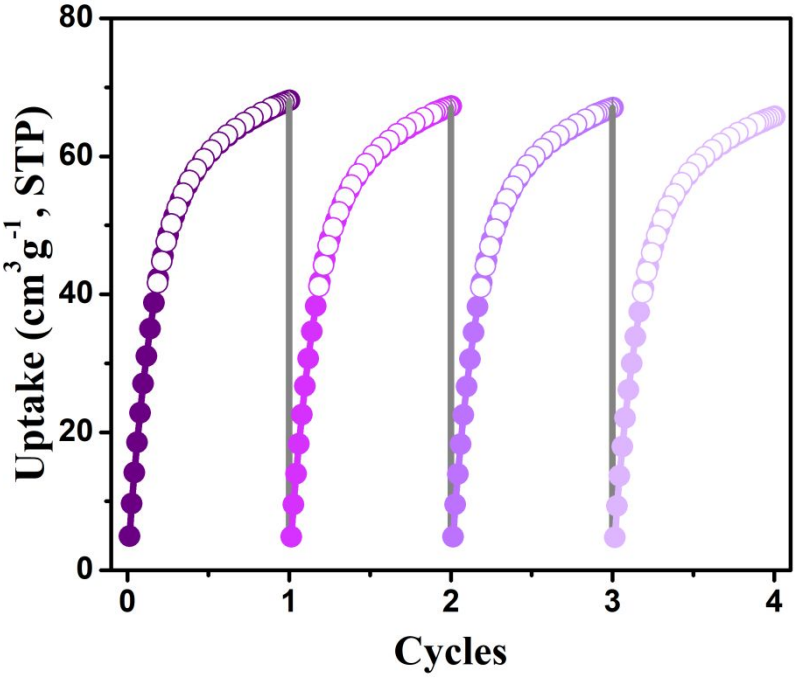

Figure S55. Sorption cycles of C_3H_8 at 298 K for PCN-909(Tb)-NH_2.

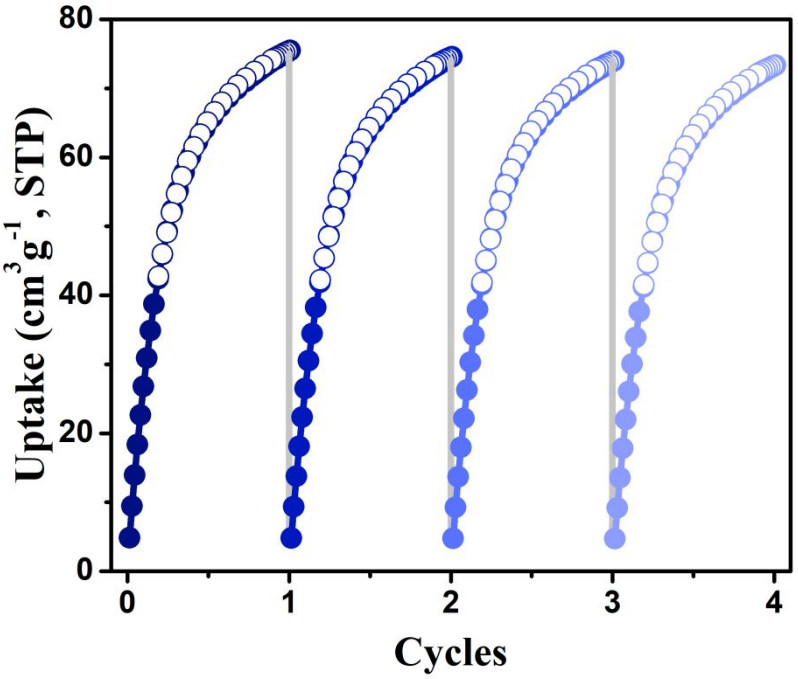

Figure S56. Sorption cycles of C_3H_6 at 298 K for PCN-909(Tb)-NH_2.

Table S3. Pore features of RE-MOFs reported in this work.

MOF	N_2 Uptake (cm^3/g)	BET surface area (m^2/g)	Langmuir surface area (m^2/g)	Experimental Pore Volume (cm^3/g)	Calculated Pore Volume (cm^3/g)
PCN-909(Eu)-Cl	231.551	661.231	928.368	0.540888	0.581435
PCN-909(Tb)-NH_2	220.525	608.460	891.392	0.502917	0.57036
PCN-912(Eu)-CH_3(50%)	291.601	828.974	1163.723	0.553440	0.686914
PCN-918(Eu)	225.904	673.381	942.054	0.381281	0.492739
PCN-918(Tb)	220.553	669.613	928.760	0.362960	-
PCN-918(Tb)-OCH_3	208.334	601.789	879.263	0.333959	-

Table S4. C_2H_6, C_2H_4, C_2H_2, C_3H_8, and C_3H_6 sorption capacity (cm^3g^{-1}) of RE-MOFs reported in this work at 273 K.

MOF	C_2H_2	C_2H_4	C_2H_6	C_3H_6	C_3H_8
PCN-909(Eu)-Cl	44.776	31.468	39.054	64.390	55.595
PCN-909(Tb)-Cl	42.454	29.949	36.473	60.494	52.576
PCN-909(Tb)-NH_2	66.369	47.594	58.722	87.885	78.239
PCN-918(Eu)	75.903	57.212	62.776	77.006	72.006
PCN-918(Tb)	80.853	60.769	68.155	84.413	75.556
PCN-918(Tb)-OCH_3	64.982	54.675	65.515	83.911	73.602
PCN-912(Tb)-CH_3(50%)	92.971	65.181	77.006	102.911	93.8868

Table S5. C_2H_6, C_2H_4, C_2H_2, C_3H_8, and C_3H_6 sorption capacity (cm^3g^{-1}) of RE-MOFs reported in this work at 298 K.

MOF	C_2H_2	C_2H_4	C_2H_6	C_3H_6	C_3H_8
PCN-909(Eu)-Cl	30.916	23.642	28.282	56.838	51.492
PCN-909(Tb)-Cl	30.678	21.782	26.998	53.122	48.352
PCN-909(Tb)-NH_2	35.700	28.798	35.542	75.478	68.096
PCN-918(Eu)	57.495	47.900	56.650	68.320	67.754
PCN-918(Tb)	57.011	47.120	56.045	75.577	73.372
PCN-918(Tb)-OCH_3	41.295	37.352	48.191	75.870	67.785
PCN-912(Tb)-CH_3(50%)	62.637	46.071	58.138	99.505	88.5248

Table S6. Pore features of reported RE_6 or RE_9- based MOFs.

MOF	N_2 Uptake (cm^3/g)	BET surface area (m^2/g)	Langmuir surface area (m^2/g)	Pore Volume (cc/g)	
Y-shp-MOF-1	543	2120	2340	0.84	5
Tb-shp-MOF-1	390	1430	1660	0.61	5
gea-MOF-1	460(Ar)	1490	1600	0.58	6
PCN-900(Eu)-NiTCPP	645	2523	-	1.01	7
ZIF-412	560	1520	2500	-	8
Tb-pek-MOF-1	220.553	1330	-	0.47	9
Y-pek-MOF-1	208.334	1608	-	0.58	9
Eu-1,4-NDC-fcu-MOF	150(Ar)	465	-	0.19	10
Tb-1,4-NDC-fcu-MOF	140(Ar)	425	-	0.18	10
Y-1,4-NDC-fcu-MOF	175(Ar)	546	-	0.22	10
Y-ftw-MOF-2	950(Ar)	3690	3740	1.26	11
Y-ftw-MOF-2(Naphth)	800(Ar)	3040	3100	1.05	11
Y-ftw-MOF-2(Anth)	610(Ar)	2100	2500	0.79	11

Table S7. C_2H_6, C_2H_4, C_2H_2, C_3H_8, and C_3H_6 sorption capacity (cm^3g^{-1}) of reported RE_6 or RE_9- based MOFs at 298 K.

MOF	C_2H_2	C_2H_4	C_2H_6	C_3H_6	C_3H_8	
gea-MOF-1	-	-	134.4	-	145.6	6
Tb-pek-MOF-1	-	-	105.28	-	109.76	9
Eu-1,4-NDC-fcu-MOF	-	-	52.64	-	45.92	10
Y-ftw-MOF-2	-	-	302.4	-	300.16	11

Table S8. Adsorption selectivity of hydrocarbon at 1 bar and 298K for different molar fraction (50:50) of binary mixtures.

MOF	C_2H_6/CH_4	C_2H_4/CH_4	C_2H_2/CH_4	C_3H_8/CH_4	
FJI-C1		9.8	39.3	78.7	12
$\{(CoCl_4)_{0.25}[Co_3(\mu_3\text{-OH})(CPT)_{4.5}](DMA)_5(DEF)\text{-}(CH_3CN)_6\}_n$			20.3		13
FJI-C4	39.7	22.1	51.0	293.4	14
$[Zn_3(dbba)_2(bipy)(DMF)]\cdot 3DMF\cdot 4H_2O$		7			15
$[Zn(dcpy)]\cdot 1.5DMF\cdot 1.5H_2O$		10			15
$[Zn(dcpy)]\cdot 1.5DMF\cdot 1.5H_2O$		7			15
$[Cu_6(L)_3(H_2O)_4(HCOO)]\cdot Me_2NH_2^+\cdot 20DMF$			33.7		16
$[Zn_2(bdc)_2(bpNDI)]\cdot 4DMF$	175	22	469		17
$Cu_2(pbpta)$	~15	~12			18
ZJU-30a	19.5	11.5	9.58		19
ZJU-31a	23.4	22.0	22.5		20
7-BPDC		189	120		21
$[Cu_2(L)\cdot(H_2O)_2]\cdot 2H_2O\cdot 3DMA\cdot(CH_3)_2NH_2$	32.2	24.1	10.3	127	22
FJU-53-Cl-a	21.5	34.1	1306		23
JLU-Liu22	14.4			271.5	24
JLU-Liu31	12			573	25
JLU-Liu40	21			845	26
UPC-33	9.94	4.78	5.78	49.18	27
PCN-909(Tb)-NH_2	11.67	8.37	9.75	53.39	This work
PCN-912(Eu)-CH_3	13.27	8.94	12.06	82.81	This work

S8. Thermogravimetric Analysis

For thermogravimetric analysis, about 10 mg of the sample was heated on a TGA/DSC1 (Mettler-Toledo) thermogravimetric analyzer from 40 to 900 °C at a rate of 10 °C·min^{-1} under N_2 flow of 50 mL·min^{-1}.

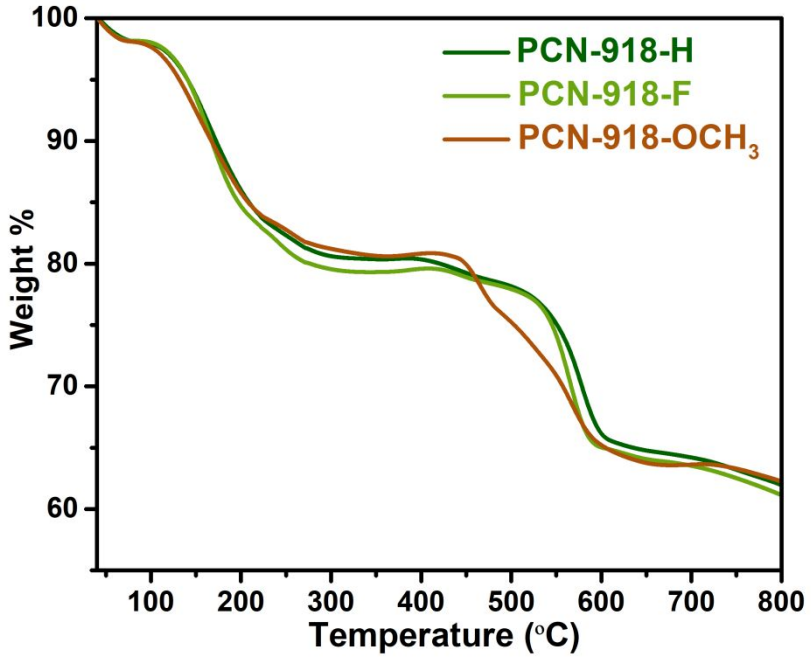

Figure S57. TGA plots of PCN-918(Eu)-H, -F and -OCH_3.

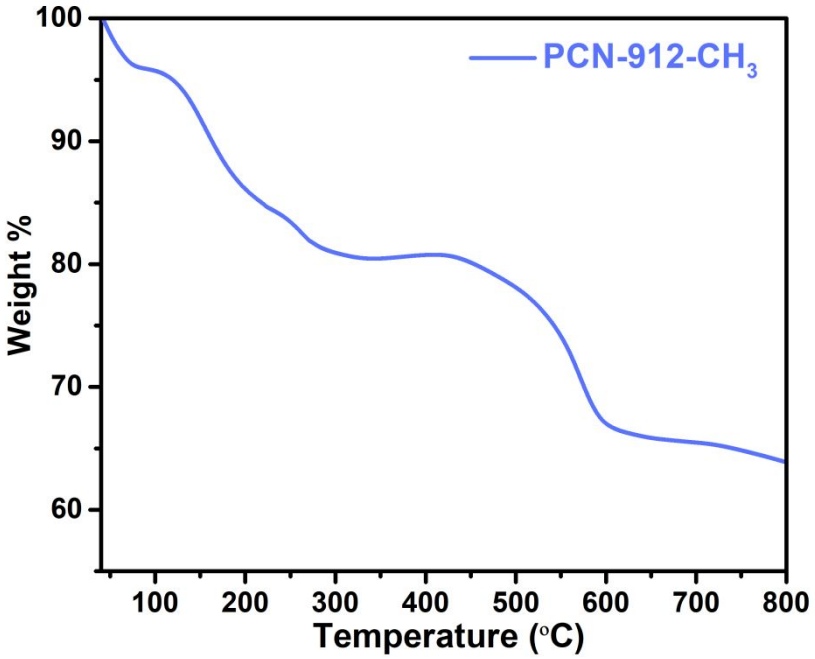

Figure S58. TGA plot of PCN-912(Eu)-CH_3.

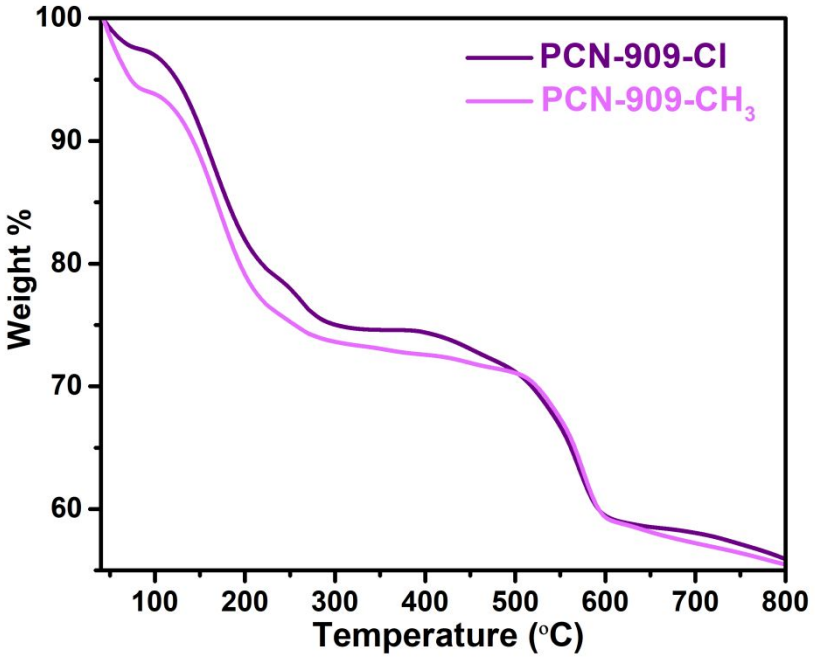

Figure S59. TGA plots of PCN-909(Eu)-Cl and -CH_3.

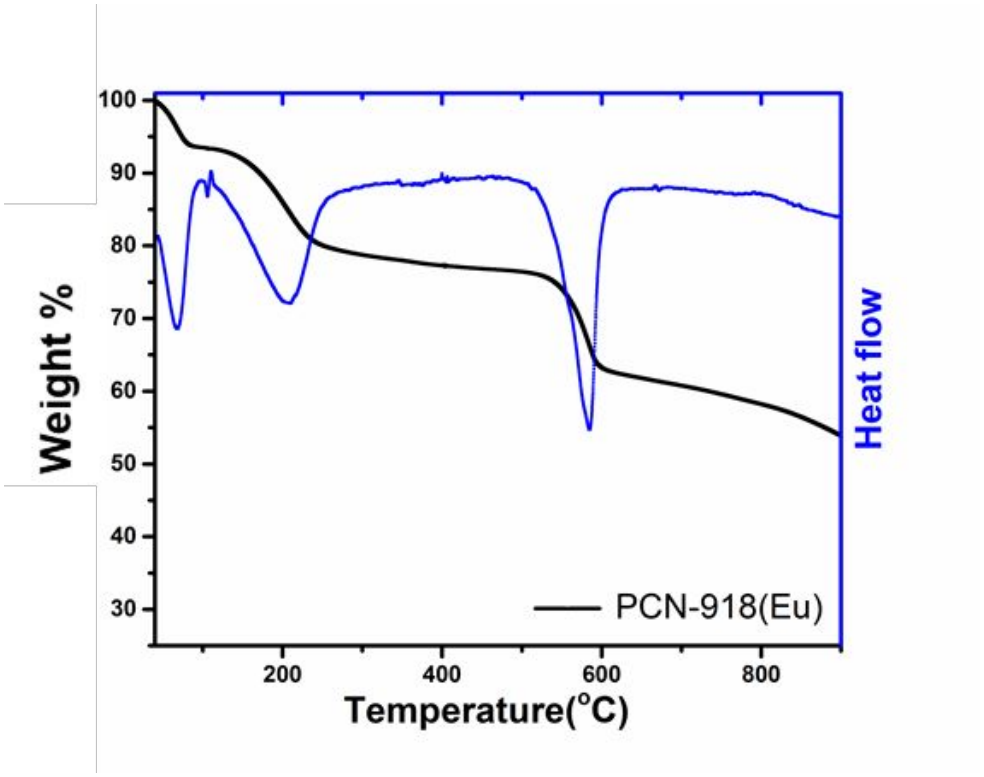

Figure S60. TGA-DSC plot of PCN-918(Eu).

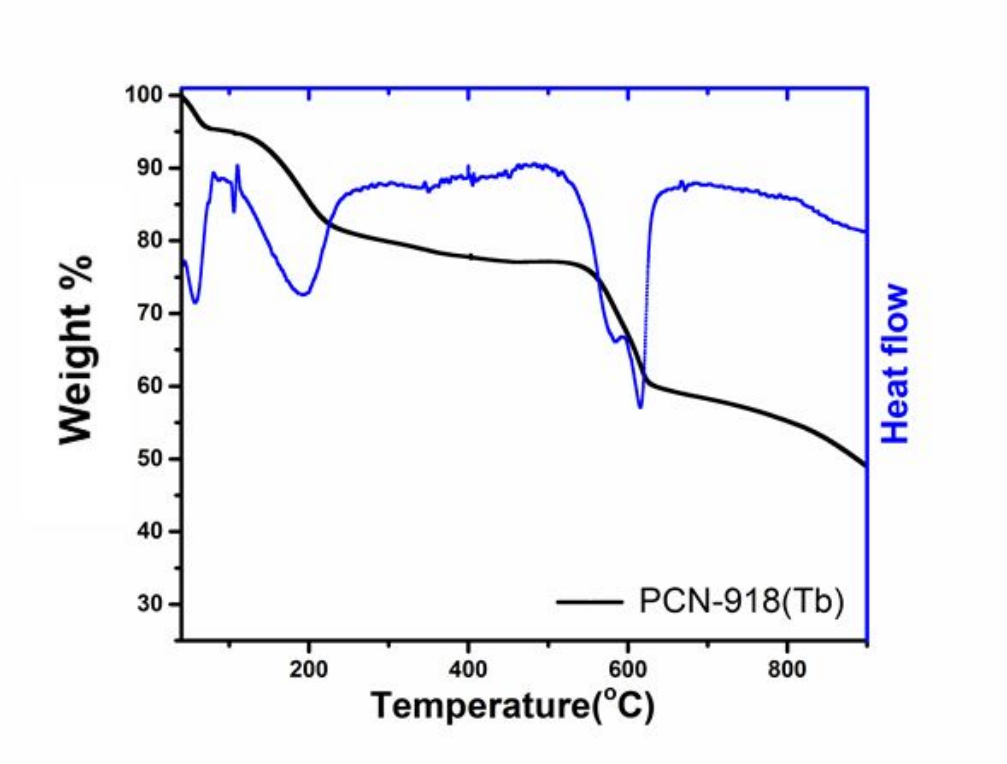

Figure S61. TGA-DSC plot of PCN-918(Tb).

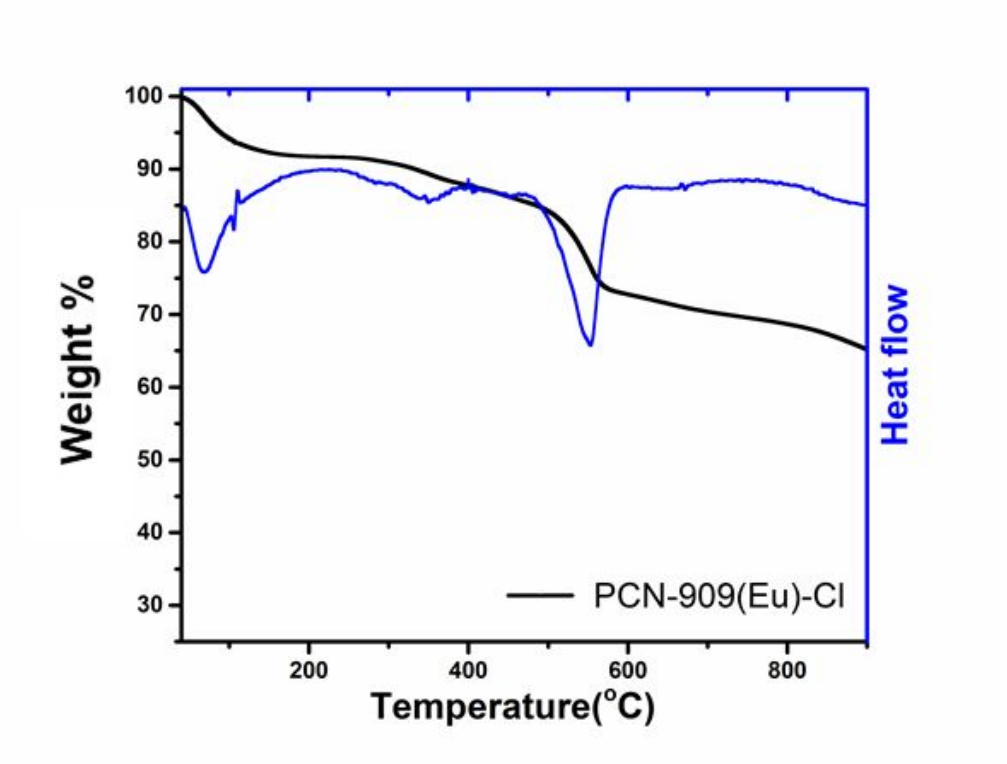

Figure S62. TGA-DSC plot of PCN-909(Eu)-Cl.

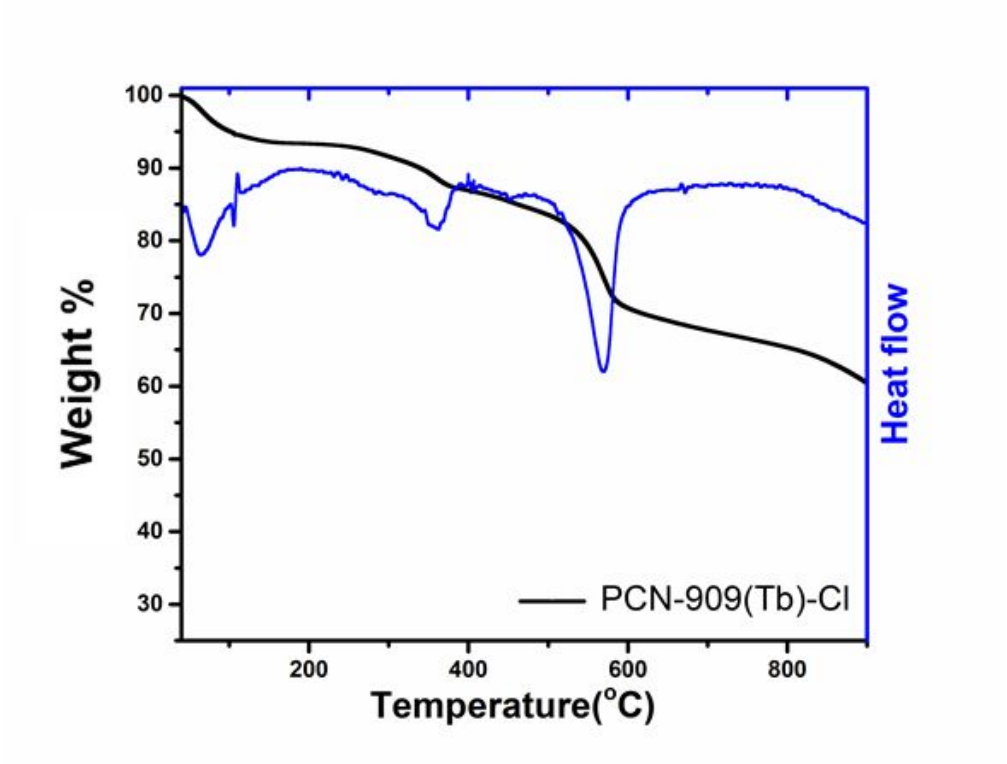

Figure S63. TGA of plot PCN-909(Tb)-Cl.

S9. ^{1}H NMR Spectroscopy

For ^{1}H NMR spectroscopy, the dry samples (around 5 mg) were digested by 10 M HCl aqueous solution and dried in 100 °C oven. The solid was dissolved in about 0.5 mL DMSO-d_6.

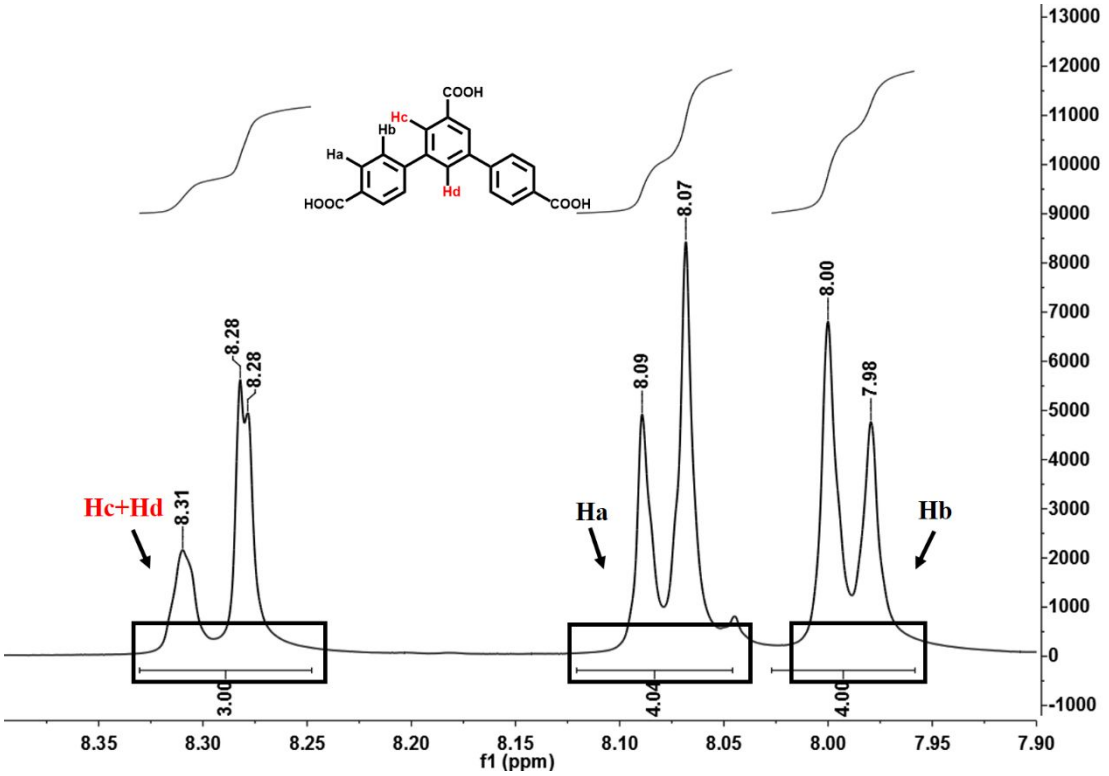

Figure S64. [1]H NMR spectroscopy of digested PCN-918(Eu).

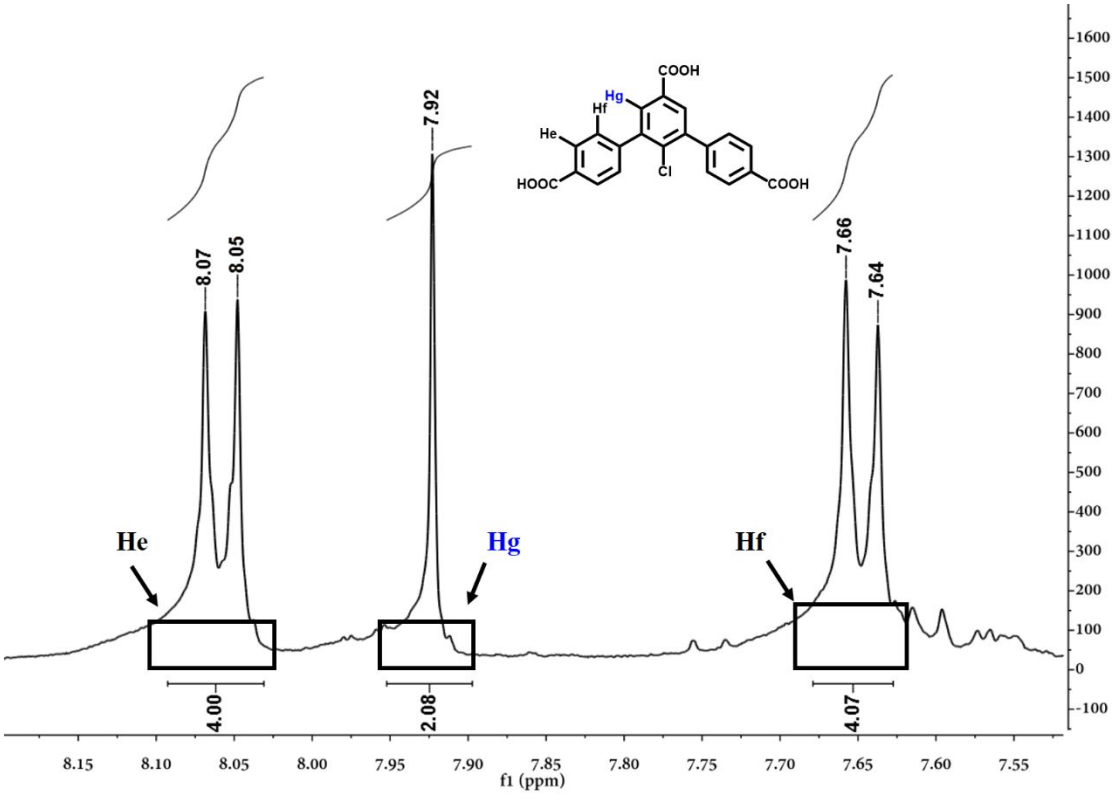

Figure S65. [1]H NMR spectroscopy of digested PCN-909(Eu)-Cl.

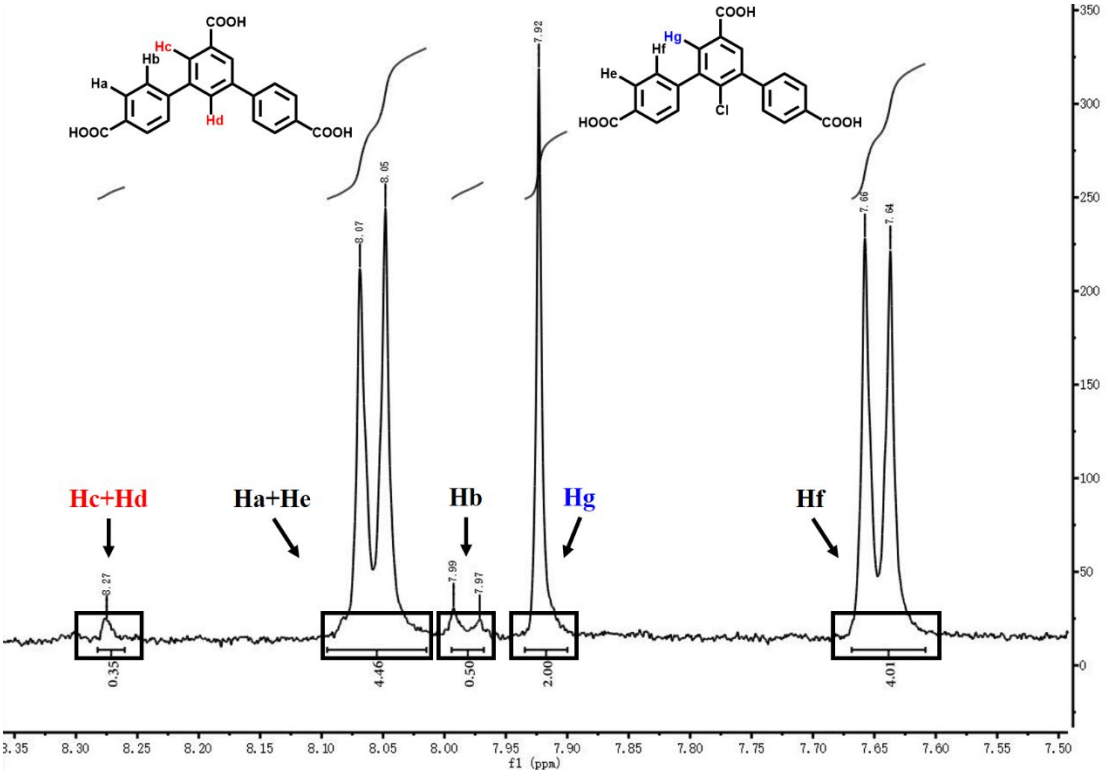

Figure S66. ^{1}H NMR spectroscopy of digested PCN-909(Eu)-Cl-65%.

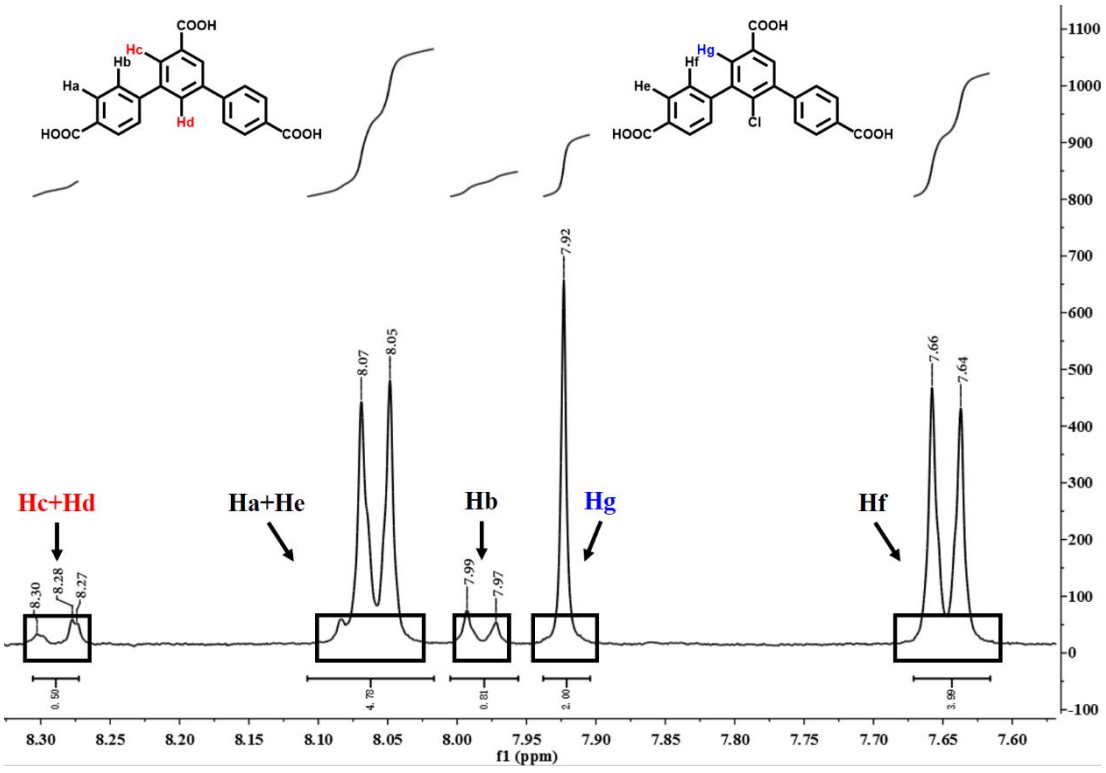

Figure S67. [1]H NMR spectroscopy of digested PCN-909(Eu)-Cl-50%.

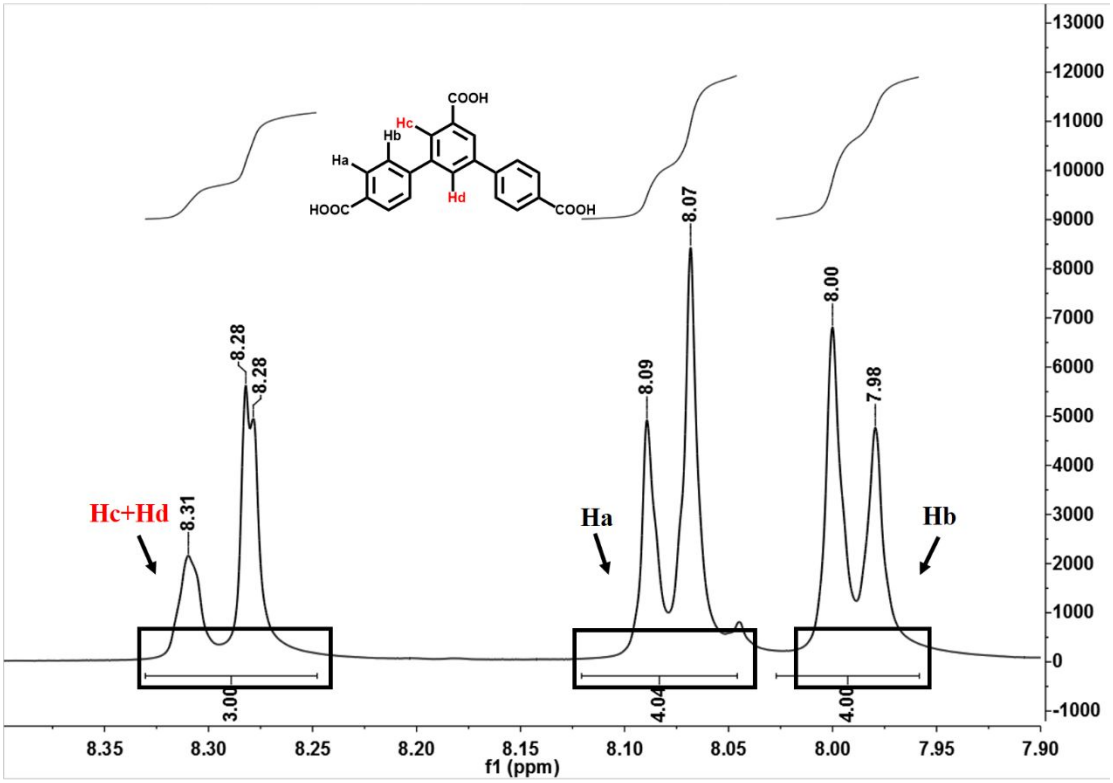

Figure S68. [1]H NMR spectroscopy of digested PCN-918(Eu)-H.

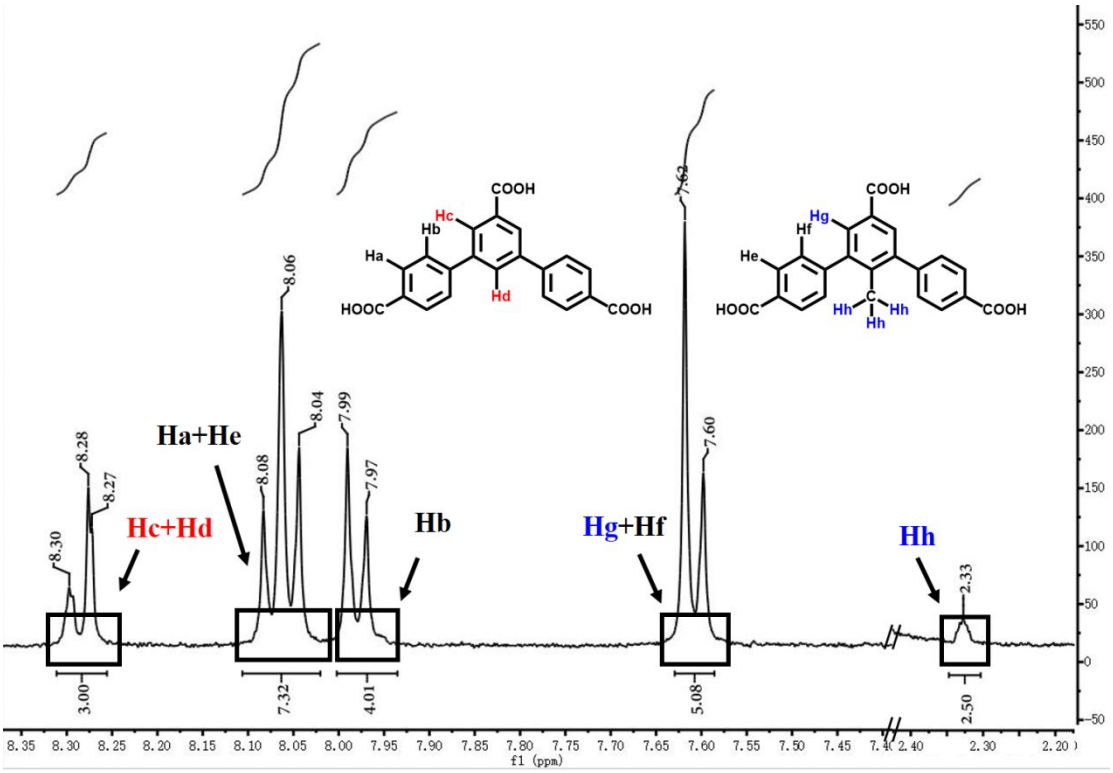

Figure S69. [1]H NMR spectroscopy of digested PCN-912(Eu)-CH_3-65%.

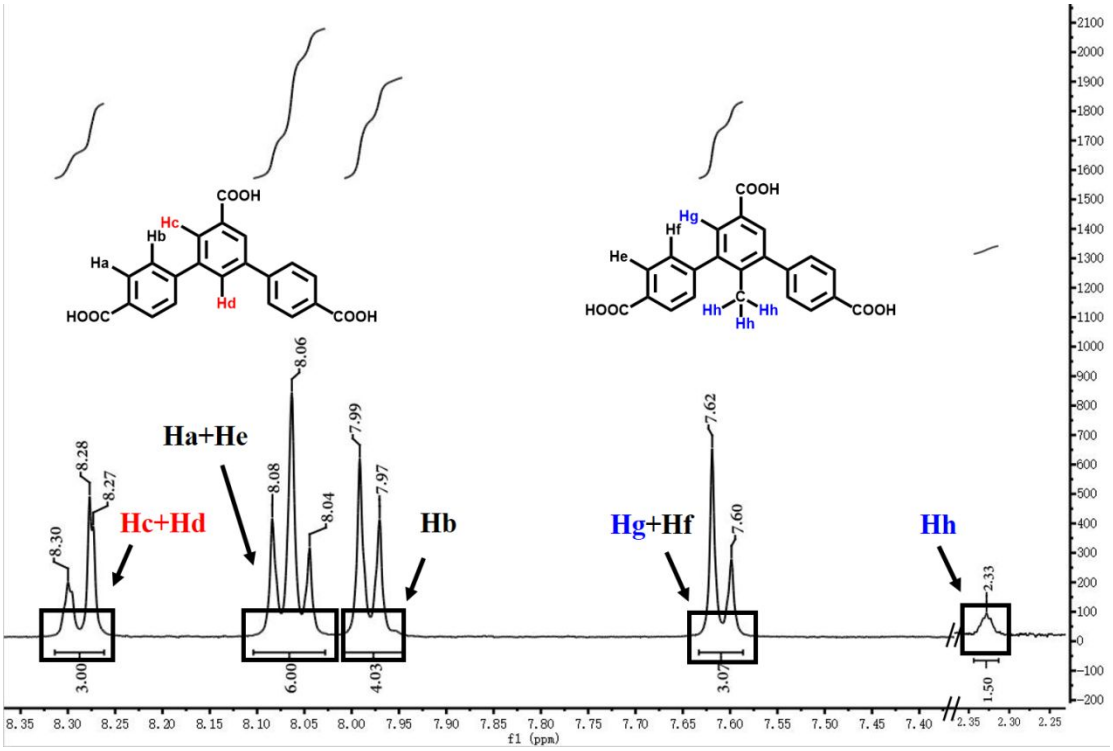

Figure S70. ^{1}H NMR spectroscopy of digested PCN-912(Eu)-CH_3-50%.

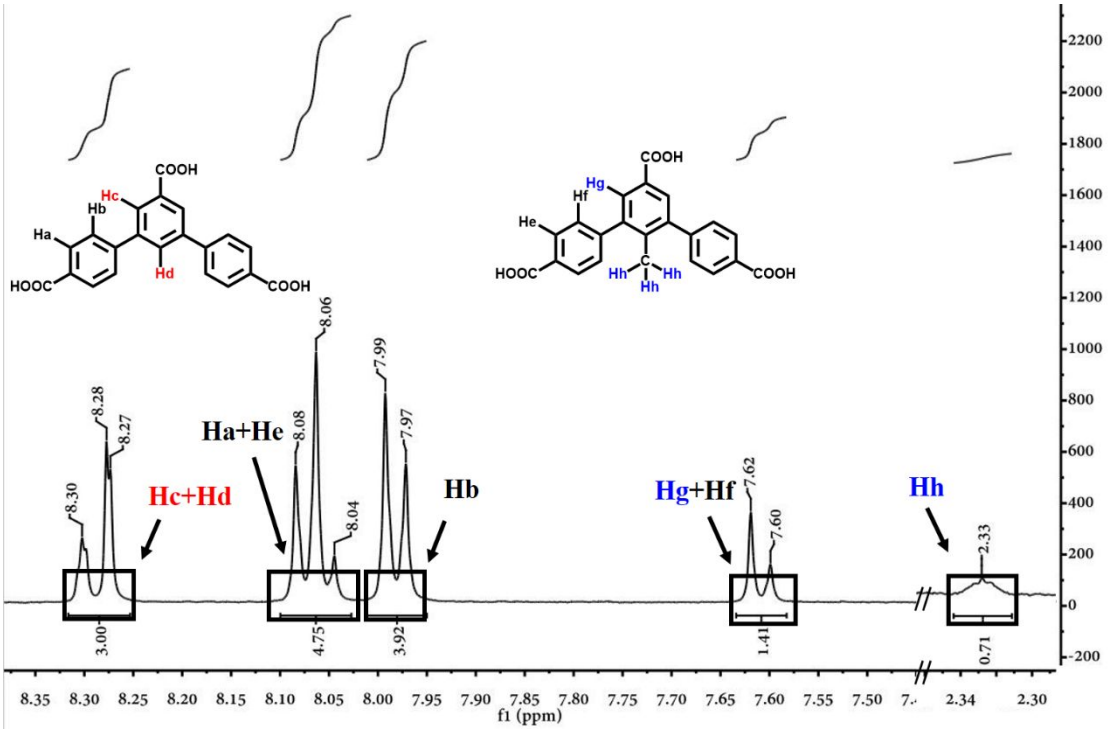

Figure S71. ^{1}H NMR spectroscopy of digested PCN-912(Eu)-CH_3-35%.

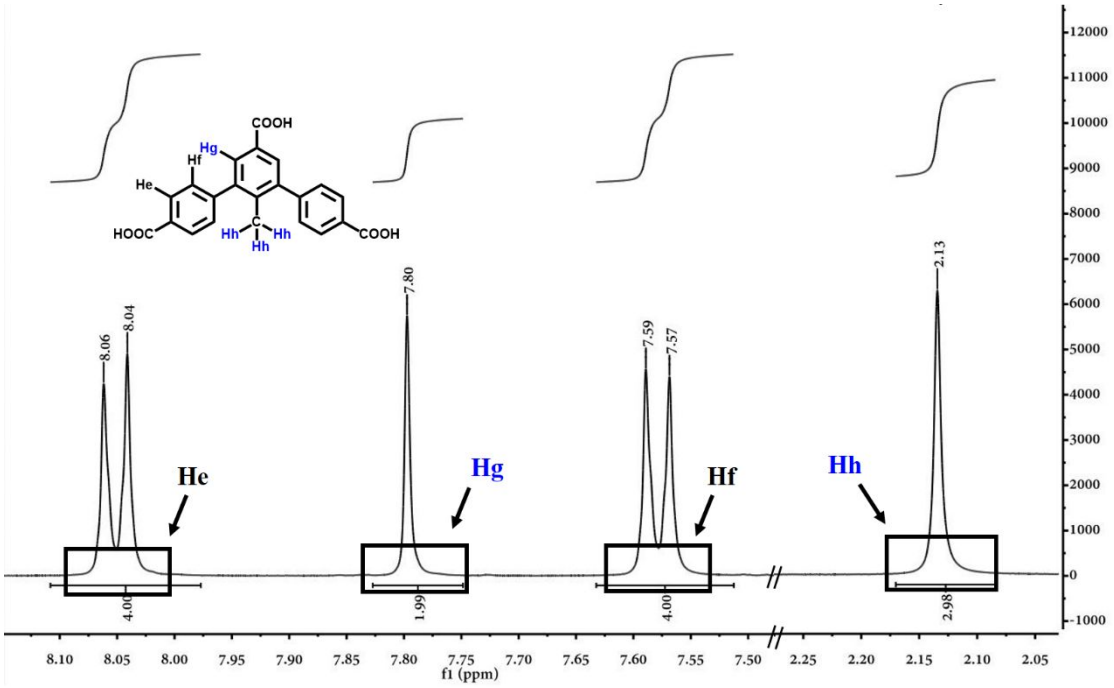

Figure S72. ^{1}H NMR spectroscopy of PCN-909(Eu)-CH_3.

Table S9. Comparison of linker ratios from starting material preparation and from ^{1}H NMR of digested sample.

MOF	Linker ratios from starting material preparation	Linker ratios from ^{1}H NMR of digested sample
PCN-909(Eu)-Cl-65%	L-H : L-Cl = 35 : 65	L-H : L-Cl = 11 : 89
PCN-909(Eu)-Cl-50%	L-H : L-Cl = 50 : 50	L-H : L-Cl = 15 : 85
PCN-912(Eu)-CH_3-65%	L-H : L-CH_3 = 35 : 65	L-H : L-CH_3 = 54 : 46
PCN-912(Eu)-CH_3-50%	L-H : L-CH_3 = 50 : 50	L-H : L-CH_3 = 67 : 33
PCN-912(Eu)-CH_3-35%	L-H : L-CH_3 = 65 : 35	L-H : L-CH_3 = 81 : 19

References

(1) Fan, W. D.; Wang, Y. T.; Xiao, Z. Y.; Zhang, L. L.; Gong, Y. Q.; Dai, F. N.; Wang, R. M.; Sun, D. F., *Inorg. Chem.* **2017,** *56*, 13634-13637.

(2) Sheldrick, G. M., *SHELXTL*, Version 6.14, Structure Determination Software Suite, Bruker AXS, Madison, WI, 2003.

(3) (a) Delley, B., *J. Chem. Phys.* **1990,** *92*, 508-517; (b) Delley, B., *J. Chem. Phys.* **2000,** *113*, 7756-7764.

(4) Perdew, J. P.; Burke, K.; Ernzerhof, M., *Phys. Rev. Lett.* **1996,** *77*, 3865-3868.

(5). Chen, Z. J.; Weselinski, L. J.; Adil, K.; Belmabkhout, Y.; Shkurenko, A.; Jiang, H.; Bhatt, P. M.; Guillerm, V.; Dauzon, E.; Xue, D. X.; O'Keeffe, M.; Eddaoudi, M., *J. Am. Chem. Soc.* **2017**, 139 (8), 3265-3274.

(6). Guillerm, V.; Weselinski, L. J.; Belmabkhout, Y.; Cairns, A. J.; D'Elia, V.; Wojtas, L.; Adil, K.; Eddaoudi, M., *Nat. Chem.* **2014**, 6 (8), 673680.

(7). Zhang, L. L.; Yuan, S.; Feng, L.; Guo, B. B.; Qin, J. S.; Xu, B.; Lollar, C.; Sun, D. F.;

Zhou, H. C., *Angew. Chem. Int. Ed.* **2018**, 57 (18), 5095-5099.
(8). Yang, J. J.; Zhang, Y. B.; Liu, Q.; Trickett, C. A.; GutierrezPuebla, E.; Monge, M. A.; Cong, H. J.; Aldossary, A.; Deng, H. X.; Yaghi, O. M., *J. Am. Chem. Soc.* **2017**, 139 (18), 6448-6455.
(9). Alezi, D.; Peedikakkal, A. M. P.; Weselinski, L. J.; Guillerm, V.; Belmabkhout, Y.; Cairns, A. J.; Chen, Z. J.; Wojtas, L.; Eddaoudi, M., *J. Am. Chem. Soc.* **2015**, 137 (16), 5421-5430.
(10). Xue, D. X.; Belmabkhout, Y.; Shekhah, O.; Jiang, H.; Adil, K.; Cairns, A. J.; Eddaoudi, M., *J. Am. Chem. Soc.* **2015**, 137 (15), 5034-5040.
(11). Luebke, R.; Belmabkhout, Y.; Weselinski, L. J.; Cairns, A. J.; Alkordi, M.; Norton, G.; Wojtas, L.; Adil, K.; Eddaoudi, M., *Chem. Sci.* **2015**, 6 (7), 4095-4102.
(12). Huang, Y.; Lin, Z.; Fu, H.; Wang, F.; Shen, M.; Wang, X.; Cao, R., *ChemSusChem*, **2014**, 7(9):2647-2653.
(13). Chen, D. M.; Zhang, N. N.; Tian, J. Y.; Liu, C. S.; Du, M., *Inorg. Chem.*, **2017**, 56(13), 7328-7331.
(14). Li, L.; Wang, X.; Liang, J.; Huang, Y.; Li, H. F.; Lin, Z. J.; Cao, R., *ACS Appl. Mater. Inter.*, **2016**, 8, 9777−9781.
(15). Zhou, H. F.; Liu, B.; Wang, H. H.; Hou, L.; Zhang, W. Y.; Wang, Y. Y., *Inorg. Chem.*, **2017**, 56(15), 9147-9155.
(16). Liu, Z.; Lv, L.; He, Y.; Feng, Y., *CrystEngComm*, **2017**, 19(20):2795 –2801.
(17). Sikdar, N.; Bonakala, S.; Haldar, R.; Balasubramanian, S.; Maji, T. K., *Chem. Eur. J.*, **2016**, 22(17), 6059-6070.
(18). Verma, G.; Kuma, S.; Pham, T.; Niu, Z.; Wojtas, L.; Perman, J. A.; Chen, Y. S.; Ma, S., *Cryst. Growth Des.*, **2017**, 17(5), 2711-2717.
(19). Cai, J.; Yu, J.; Xu, H.; He, Y.; Duan, X.; Cui, Y.; Wu, C.; Chen, B.; Qian, G., *Cryst. Growth Des.*, **2013**, 13(5), 2094-2097.
(20). Cai, J.; Yu, J.; Wang, H.; Duan,X.; Zhang, Q.; Wu, C.; Cui, Y.; Yu, Y.; Wang, Z.; Chen, B.; Qian, G., *Cryst. Growth Des.*, **2015**, 15(8), 4071-4074.
(21). Zhai, Q. G.; Bai, N.; Li, Shuni; Bu, X.; Feng, P., *Inorg. Chem.*, **2015**, 54(20), 9862-9868.
(22). Liu, X.; Li, X.; Li, J.; Li, G.; Guo, S.; Zhu, H.; Zhao, Li.; Hao, C.; Guo, W., *J. Mater. Sci.*, **2018**, 53(12), 8866-8877.
(23). Wang, L.; Ye, Y.; Li, Z.; Lin, Q.; Ouyang, J.; Liu, L.; Zhang, Z.; Xiang, S., *Cryst. Growth Des.*, **2017**, 17(4), 2081-2089.
(24). Wang, D.; Liu, B.; Yao, S.; Wang, T.; Li, G.; Huo, Q.; Liu, Y., *Chem. Comm.*, **2015**, 51(83), 15287-15289.
(25). Yao, S.; Sun, X.; Liu, B.; Krishna, R.; Li, G.; Huo, Q.; Liu, Y., *J. Mater. Chem. A*, **2016, 4**(39), 15081-15087.
(26). Sun, Q.; Yao, S.; Liu, B.; Liu, X.; Li, G.; Liu, X.; Liu, Y., *Dalton Trans.*, **2018**, 47(14), 5005-5010.
(27). Fan, W. D.; Wang, Y. T.; Zhang, Q.; Kirchon, A.; Xiao, Z. Y.; Zhang, L. L.; Dai, F. N.; Wang, R. M.; Sun, D. F., *Chem. Eur. J.*, **2017**, 24(9), 2137-2143.